Examining the Neurovisceral Integration Model through fNIRS

Emma Elizabeth Condy

Dissertation submitted to the Faculty of the
Virginia Polytechnic Institute and State University
in partial fulfillment of the requirements for the degree of

Doctor of Philosophy
in
Psychology

Bruce H. Friedman, Chair
Martha Ann Bell
Rachel A. Diana
Amir H. Gandjbakhche
John A. Richey

August 2, 2018
Blacksburg, VA

Keywords: respiratory sinus arrhythmia, behavioral inhibition, neurovisceral integration, functional near-infrared spectroscopy

Examining the Neurovisceral Integration Model through fNIRS

Emma Elizabeth Condy

Abstract

The neurovisceral integration model (NVM) proposes that an organism's ability to flexibly adapt to their environment is related to biological flexibility within the central autonomic network. One important aspect of this flexibility is behavioral inhibition (Thayer & Friedman, 2002). During a behavioral inhibition task, the central autonomic network (CAN), which is comprised of a series of feedback loops, must be able to integrate information and react to these inputs flexibly to facilitate optimal performance. The functioning of the CAN is shown to be associated with respiratory sinus arrhythmia (RSA), as the vagus nerve is part of this feedback system. While the NVM has been examined through neural imaging and RSA, only a few studies have examined these measures simultaneously during the neuroimaging procedure. Furthermore, these studies were done at rest or used tasks that were not targeted at processes associated with the NVM, such as behavior inhibition and cognitive flexibility. For this reason, the present study assessed RSA and neural activation in the prefrontal cortex simultaneously while subjects completed a behavior inhibition task. Using a series of go/no-go tasks, RSA and functional near-infrared spectroscopy (fNIRS) were collected to investigate the relationship between prefrontal activation and vagal activity at rest and during behavioral inhibition.

There are three primary aims of this study. First, examine prefrontal activation during various inhibition tasks through fNIRS. Second, evaluate the NVM during a cognitive task using simultaneous fNIRS and RSA analysis. Third, relate task performance, imaging, and RSA measures during behavioral inhibition to deficits in flexible everyday responding, as indicated by self-report measures of behavior. Doing so will elucidate the connection with prefrontal

activation and RSA as proposed by the NVM model and determine whether neural and RSA metrics can be related to broader symptoms of inflexibility.

Examining the Neurovisceral Integration Model through fNIRS

Emma Elizabeth Condy

General Audience Abstract

The neurovisceral integration model (NVM) proposes that the ability to adapt to the environment is related to biological flexibility within the brain. One important aspect of the ability to adapt to the environment is behavior inhibition (e.g., the ability to stop from engaging in a habitual response, Thayer & Friedman, 2002). During a behavior inhibition task, the brain must be able to integrate information and react to these inputs flexibly to facilitate optimal performance. The brain's ability to do this is related to a measure of heart activity known as respiratory sinus arrhythmia (RSA). The present study assessed RSA and brain activity while subjects completed a behavior inhibition task. Neural activation was measured through functional near-infrared spectroscopy (fNIRS). fNIRS measures the amount of oxygenated blood in different areas of the brain. Greater concentrations of oxygenated blood indicated greater brain activity in an area. Through simultaneous fNIRS and RSA measurement the present study examined their relationship during various inhibition tasks. Doing so clarified the connection between brain activation and RSA as proposed by the NVM model.

Table of Contents

List of abbreviations

ACC:	anterior cingulate cortex
AQ:	Autism-Spectrum Quotient
BA:	Brodmann area
CAN:	central autonomic network
CFI:	Cognitive Flexibility Inventory
DMN:	Default mode network
ECG:	electrocardiogram
EF:	executive function
fMRI:	functional magnetic resonance imaging
fNIRS:	functional near-infrared spectroscopy
GNG:	go/no-go
HHb:	deoxygenated hemoglobin
HRV:	heart rate variability
IBI:	interbeat interval
ISI:	interstimulus interval
HFHRV:	high frequency heart rate variability
mPFC:	medial prefrontal cortex
NVM:	neurovisceral integration model
O_2Hb:	oxygenated hemoglobin
PFC:	prefrontal cortex
PNS:	parasympathetic nervous system
RMSSD:	root mean square successive differences
RBQ-2A:	Repetitive Behavior Questionnaire, Adult
RSA:	respiratory sinus arrhythmia
SA:	sinoatrial
SMA:	supplementary motor area
SNS:	sympathetic nervous system
vmPFC:	ventromedial prefrontal cortex

Examining the Neurovisceral Integration Model through fNIRS

The autonomic nervous system (ANS) regulates the activity of organ systems that are key to precise coordination of body functioning. The principal role of the ANS is to maintain the body's internal environment by distributing and integrating specific signals to target organs (Janig & Habler, 2000). The ANS is traditionally divided into two branches: the parasympathetic (PNS) and sympathetic (SNS), which have anatomical, functional, and neurochemical distinctions[1].

The *neurovisceral integration model* (NVM) proposes that these systems are part of the central autonomic network (CAN) (Thayer & Lane, 2000), which operates through a series of feedback loops within the central nervous system. These feedback loops include both central and peripheral inputs and outputs and subsequently influence a number of behavioral and physiological processes. Importantly, measurements of the peripheral outputs of this system can be used to index the functionality of feedback loops in the CAN. Structures within the CAN include many regions throughout the brain; however, those in the cortex are of interest in the present study. Cortical structures in the CAN that are highlighted in the NVM include the medial prefrontal cortex (mPFC), anterior cingulate cortex (ACC), and the insula (Benarroch, 1993). The NVM proposes that cortical structures, such as the mPFC, institute tonic inhibition on activation of the amygdala, resulting in heightened CAN output (Thayer, Hansen, Saus-Rose, & Johnsen, 2009). This view is based on evidence from animal studies as well as human neuroimaging, which has established structural interconnections, and pharmacological studies, in which both branches of the ANS are blocked and show increased activation compared to the

[1] A third *enteric* branch, which innervates the gastrointestinal organs, is sometimes also distinguished; see Janig & Habler (2000).

normal state, indicating that the system is under tonic inhibitory influence (Thayer et al., 2009). One of the outputs of the CAN is the vagus nerve, which innervates the heart. For this reason, respiratory sinus arrhythmia (RSA), an index of vagal activation derived from the electrical signal of the heart, is commonly used to provide information about the functionality of the CAN.

The electrocardiogram (ECG) provides information about the electrical activity of the heart, allowing various elements of the cardiac cycle to be measured, such as the duration of interbeat intervals (IBIs). The variation from beat-to-beat in these intervals, known as heart rate variability (HRV), is controlled by SNS and PNS inputs to the sinoatrial (SA) node of the heart (Task Force, 1996). SNS input to the SA node is excitatory, and PNS input (via the vagus nerve) is inhibitory. When PNS activity to the SA node increases (and SNS activity remains constant), IBIs will lengthen. Furthermore, differences in the temporal dynamics of the primary neurotransmitters involved in SNS and PNS activation (norepinephrine and acetylcholine, respectively) allow fast changes in IBI length to be attributed to PNS activation (Saul, 1990). RSA refers specifically to changes in the lengths of IBIs as a result of respiration, with inspiration causing the shortening of IBIs and expiration causing in the lengthening of IBIs (Berntson, Cacioppo, & Quigley, 1993). This variability can be quantified through either a frequency-based metric, which uses a power analysis to measure changes within the high-frequency band (quantified at the frequency of respiration (0.12-0.40 Hz) and known as high frequency heart rate variability (HFHRV)) (J. J. Allen, Chambers, & Towers, 2007), or through a time-based metric, which quantifies changes from beat-to-beat using the root mean square successive difference (RMSSD) (Berntson et al., 1997).

Both metrics are used to quantify RSA, which indexes CAN function. It is posited in the NVM that high baseline RSA and increased RSA reactivity are indicative of increased flexibility

within the CAN (Friedman, 2007). The flexibility within this biological system is also said to be manifested through greater cognitive and behavioral flexibility, which is evidenced by skills such as better emotional regulation and inhibitory capacities.

The aim of the present study was to further evaluate the claims of the NVM through simultaneous measurement of RSA and cortical activation. Though previous studies have looked at RSA in relation to brain activity, there are many limitations in the literature, such as limited sample sizes and inappropriate methodology. In the present study, prefrontal cortex activity was assessed via functional near-infrared spectroscopy (fNIRS) in concert with RSA during both baseline and cognitive tasks. This strategy was taken to apply the NVM to fNIRS data, and to further examine the relationship between CAN activation and RSA by evaluating it across various contexts. The study also explored how these metrics relate to other functional domains implicated in the NVM, namely cognitive and behavioral flexibility.

Through a review of the current state of the neuroimaging literature surrounding the NVM and its associated cognitive processes (e.g., behavioral inhibition), the present study argues that previous studies evaluating the NVM could be improved upon methodologically in both the approach to biological measurement and the selection of experimental conditions. The present study then integrates simultaneous neural and psychophysiological measurement to address these gaps in the literature. This will be achieved by measuring these variables at baseline as well as during a behavioral inhibition task (i.e., the go/no-go). Neural activation during this task, as well as its relation to RSA at rest and during active behavior inhibition will then be assessed and compared to the previous literature. The findings from the present study are then discussed in relation to the theoretical implications for the NVM and potential practical applications of the biological markers associated with the NVM and their relation to behavior inhibition abilities.

Human Neuroimaging & the Neurovisceral Integration Model

Much of the literature supporting the NVM and the relationship between HFHRV and the CAN is based on animal models and blockade studies. However, there have been several human neuroimaging studies examining the theory. These studies were reviewed in two meta-analyses, which concluded that a number of areas associated with the NVM were activated in conjunction with heightened HFHRV (Beissner, Meissner, Bar, & Napadow, 2013; Thayer, Ahs, Fredrikson, Sollers, & Wager, 2012). Specifically, HFHRV was associated with areas of the mPFC such as the right rostral PFC (Brodmann Area (BA) 10/32), and pre- and sub-genual cingulate (BA 24/32 and BA 25) (Thayer et al., 2012). Furthermore, Beissner et al. (2013) note that many of the structures associated with HFHRV in their meta-analysis are part of the *default mode network* (DMN). The DMN is comprised of brain regions that are active when an individual is not engaged in a task and is instead focused on internal events, such as self-reflection and future planning. These include the ventromedial prefrontal cortex (vmPFC) and dorsomedial prefrontal cortex (dmPFC), posterior cingulate cortex, hippocampal formation, inferior parietal lobule and lateral temporal cortex (Buckner, Andrews-Hanna, & Schacter, 2008). This is a particularly interesting point because the NVM has largely been evaluated at rest in the neuroimaging literature. The study conjectures that although the vmPFC was not shown to be significantly related to HFHRV across the studies in their meta-analysis, they suggest that the vmPFC does play a role in this feedback loop due to known connections between this area and structures that were found to be associated with HFHRV.

It should be noted that the studies included in these meta-analyses had limited sample sizes, used dissimilar methods (e.g., some baseline and others task-based measures), and incorporated HFHRV measurements that were taken at a different time than the neuroimaging

data. These are all significant limitations, but the last point is particularly concerning. These studies were based on the assumption that the baseline state during HFHRV measurement would be comparable to that of the neuroimaging data collection. Simultaneous collection of HFHRV and neuroimaging data is necessary to avoid such assumptions, which cannot be unequivocally made. Regardless, both meta-analyses revealed that baseline HFHRV values correlate with resting neural activity in areas implicated in the CAN.

Subsequent studies have further addressed some of these limitations (B. Allen, Jennings, Gianaros, Thayer, & Manuck, 2015; Jennings, Allen, Gianaros, Thayer, & Manuck, 2015). These studies show vast improvement in that they had large sample sizes; however, they also collected HFHRV data outside of the scanner and only looked at these measures at baseline. Nonetheless, the studies found that higher baseline HFHRV (taken approximately 2 weeks prior to their neuroimaging appointment) was correlated with lower cerebral blood flow at rest in the left insula (BA 13), right hippocampus, and right superior temporal gyrus (BA 41) when controlling for age. The researchers also note that the findings, specifically the directionality of the correlations between HFHRV and neural activation, differ from those found in the meta-analyses described above. They propose that differences in HFHRV-neural relationships across different contexts, such as baseline versus task based measurement, may differentially relate to the activation of neural structures implicated in the CAN.

A related study focused on this question by incorporating performance on a series of executive function (EF) tasks related to the NVM into the analyses (Jennings et al., 2015). These analyses separately examined the relationship between baseline HFHRV and EF performance, baseline HFHRV and resting neuroimaging data, and EF performance and resting neuroimaging data. While interesting relationships between these variables were found (namely that global

cerebral blood volume was positively related to baseline HFHRV), again these components were not measured simultaneously. Furthermore, the EF tasks in this study were largely working memory tasks and consequently did not incorporate inhibition, which is the key cognitive and behavioral construct implicated in the NVM. Considering the limitations present in the extant literature, it is important for future research examining the NVM to measure HFHRV and neural activation simultaneously both at baseline and during an appropriate cognitive task.

Some studies provide insight for methodological improvements in examining RSA in conjunction with functional magnetic resonance imaging (fMRI) by implementing time series analyses that look at the two signals simultaneously. One such study examined changes in functional connectivity in relation to fluctuations in RMSSD or HFHRV during a resting state fMRI (Chang et al., 2013). Through sliding-window calculations of both the fMRI and HRV signal at certain time points, the correlation of these two signals over the course of the resting state scan was examined. Results indicated that greater functional connectivity between the dorsal anterior cingulate cortex/amygdala and the mPFC, as well as the insula are associated with heightened HFHRV. These findings reflect connections and relationships between RSA and the connectivity of structures proposed in the NVM. These results support the NVM, but they only provide information about the relationship between these variables during rest.

Another study used a point process adaptive-filter to compute HFHRV and then regressed this HFHRV time series onto the fMRI signal during a motor task (Napadow et al., 2008). Positive correlations between HFHRV and several areas associated with the NVM, including the amygdala, right dorsal mPFC, and right dorsal lateral PFC, as well as negative correlations with the left posterior insula and right medial temporal gyrus during a hand-grip task were found. The sample size was limited (N=7), and a simplistic motor task was used, but the study

simultaneously assessed RSA and neural data effectively, and in doing so provides supporting evidence for the NVM. Use of this methodological approach during a task that aligns with the psychological constructs implicated in the NVM, such as a behavioral inhibition task, would capture the neural activity associated with inhibitory processes and better elucidate how these processes relate to the CAN.

Behavioral Inhibition & Neuroimaging

One cognitive task which assesses inhibition is the go/no-go (GNG) task. This simple task was developed to assess behavioral inhibition (Donders, 1969), and now has variants which incorporate emotional stimuli (Schulz et al., 2007). The GNG is used across a variety of psychological studies to assess how behavioral inhibition relates to other functions. Furthermore, performance on the GNG is affected in many disorders characterized by inhibition deficits, such as attention deficit-hyperactivity disorder (Dillo et al., 2010), obsessive compulsive disorder (Lee, Yost, & Telch, 2009), and autism spectrum disorder (Uzefovsky, Allison, Smith, & Baron-Cohen, 2016). The task consists of two types of stimuli: the 'go' stimulus, which indicates that the subject should complete the behavioral response (e.g., a button press), and the 'no-go' stimulus, which indicates that the subject should not complete the behavioral response (e.g., no response). By prompting a prepotent response through a series of 'go' trials, the subject is then challenged to inhibit the behavior during the 'no-go' stimulus. The GNG was used in the present study to assess inhibition processes as they relate to neural and RSA measurements. Its wide use in the neuroimaging literature provides extensive information about the neural correlates of behavioral inhibition processes. These studies, in conjunction with the theory presented in the NVM, create the foundation for the hypotheses that were examined in the present study.

Functional magnetic resonance imaging (fMRI).

Many fMRI studies have examined the GNG task to assess neural activation patterns associated with inhibition. Most fMRI studies use block designs to study between-task differences; however, the use of event-related designs allows for more thorough analysis of inhibition, in that these designs allow researchers to examine neural activation during simple 'no-go' trials compared to 'go' trials. Such studies have indicated that different areas of the frontal cortex show activation specific to 'no-go' trials, such as the bilateral mPFC (BA 10) (Watanabe et al., 2002) and the pre-supplementary motor area (pre-SMA) (BA 6) (Mostofsky et al., 2003). However, meta-analyses of studies that use event-related designs during fMRI have found it difficult to identify consistent inhibition-specific areas of activation in studies using the GNG task when controlling for factors such as working memory load and attention. This issue was addressed by comparing activity during the simple GNG task to other behavioral inhibition tasks or variants of the GNG task with different levels of cognitive demand to identify activation patterns specific to inhibition. For instance, when the GNG was compared to another behavioral inhibition task (the stop-trial task) the only areas of overlapping activation were the pre-SMA and insula. However, GNG-specific activation included the right medial frontal gyrus and the right inferior parietal lobule (Swick, Ashley, & Turken, 2011). Similarly, when GNG networks were compared between complex and simple versions of the GNG, the pre-SMA and left fusiform gyrus were common to both networks (Simmonds, Pekar, & Mostofsky, 2008). However, studies were deemed simple versus complex simply based on the ratio of go to no-go trials used in the task. Conversely, another meta-analysis which examined how working memory and attention may factor into these networks identified multiple factors by which to classify GNG task complexity, including: (1) number of no-go stimuli, (2) go signal to no-go signal ratio,

and (3) working memory load. After breaking the studies down by task complexity, the authors suggest that activation in the pre-SMA may not play a direct role in inhibition, as activation in the pre-SMA appeared to be related to increased working memory load (Criaud & Boulinguez, 2013). It was concluded that there is a need for additional GNG imaging studies which utilize simple GNG paradigms, and that use appropriate event-related contrasts for analyses. These critiques are essential in formulating future studies which incorporate the GNG task. Based on these criticisms, multiple versions of the GNG task were used in the present study.

One way to vary the GNG task is through the incorporation of different 'go' and 'no-go' stimuli. Doing this allows researchers to examine how behavioral inhibition varies as a function of stimulus content, and thus across different contexts. By contrasting a simple GNG task with a more complex design, not only can changes in performance be examined (such as increased number of errors or longer reaction times), but this can also uncover areas of unique neural activation versus overlapping activation between the task types. Of specific interest in the present study was the emotional GNG, which uses pictures of faces as stimuli. Faces with neutral expressions act as a 'go' stimulus and faces with emotional expressions act as a 'no-go' stimulus (some variations of the task use neutral and emotional words instead of faces). The task requires more resources than a simple GNG task while still maintaining measurement of behavior inhibition ability like a simple GNG task (Schulz et al., 2007).

The emotional GNG is of interest in the present study due to the role of emotional stimuli in the NVM framework. In a comprehensive review of studies examining the NVM, when activation during emotional tasks was compared to cognitive tasks, differences in the activation of CAN-associated structures were found (Thayer et al., 2012). Namely, emotional tasks elicited greater activation of the right mPFC than cognitive tasks. Similarly, through an emotional GNG

task, one study found greater mPFC activation during emotional trials compared to neutral, indicating that it plays role in inhibition specifically when processing emotional stimuli (Goldstein et al., 2007). A similar study found other areas integral in the CAN, such as the right insula and subgenual cingulate (BA 32), may also be more active during emotional trials of the GNG (Elliott, Rubinsztein, Sahakian, & Dolan, 2000). These studies illustrate how different structures within the CAN are activated depending on stimulus content. Consequently, it is important to incorporate tasks which incorporate both emotional and simple stimuli when examining the NVM. For this reason, the present study used both the simple GNG and emotional GNG task in its investigation of the NVM and behavior inhibition.

Lastly, fMRI studies have shown that activation in the areas associated with successful inhibition during the simple GNG has been related to broader behavioral inhibition measures. Specifically, increased right dorsolateral PFC activity during 'no-go' trials compared to 'go' trials has been associated with lower impulsivity scores on a behavioral self-report scale (Asahi, Okamoto, Okada, Yamawaki, & Yokota, 2004), even though GNG performance did not correlate with this scale. These findings suggest that neural activation during a behavioral inhibition task affords information about daily functioning beyond that of performance on the task alone. Although there is not yet consensus in the fMRI literature regarding areas of activation specifically associated with behavioral inhibition, Asahi et al. (2004) showed that neural correlates of general inhibition ability can be detected. Therefore, activation of cortical areas during successful inhibition could correlate with other behaviors related to inhibition deficits, such as rumination, repetitive behaviors, and other cognitive and behavioral inflexibilities. These are important applications of the NVM and related research because behavioral inhibition deficits are thought to permeate many domains of functioning. Furthermore, the incorporation of

an emotional GNG provides data to examine inhibition activation as it relates to emotion processing, which could impact other domains, such as social functioning. Due to temporal and ecological limitations of fMRI technology, the present study incorporated a different imaging modality (i.e., fNIRS) to assess inhibition through the GNG task while using information afforded by the extant fMRI literature to generate an appropriate GNG task design and formulate hypotheses.

Functional near-infrared spectroscopy

fNIRS is an optical imaging technique which projects infrared light (650-1000 nm) from a source diode into tissue and measures the backscatter of this light using detectors. Based on the amount of backscatter, the concentration of oxygenated hemoglobin (O_2Hb) and deoxygenated hemoglobin (HHb) can be determined because O_2Hb and HHb have different optical properties (Ferrari & Quaresima, 2012). Though originally used to image various tissues *in vivo*, this technology has been developed into imaging equipment designed to measure oxygenation across the cerebral cortex in humans. fNIRS has some advantages over fMRI as a neuroimaging technology. Not only does fNIRS have higher temporal resolution, which better lends itself to event-related designs, there is also less concern about motion artifact interfering with the signal (Irani, Platek, Bunce, Ruocco, & Chute, 2007; Lloyd-Fox, Blasi, & Elwell, 2010). The relative immunity to motion artifact compared to fMRI is particularly important because fNIRS allows for subject movement and thus affords greater ecological validity and task flexibility. These features afford more options when designing tasks to be used during neuroimaging. For these reasons, fNIRS is a valuable technique for collecting neuroimaging data from the cortex during task-based studies of cognition and behavior.

Though there are many benefits of using fNIRS in studies that examine cognition through behavioral paradigms, fewer studies using fNIRS during the GNG task have been conducted compared to fMRI. Similar to fMRI findings, fNIRS studies have shown increased O_2Hb in the prefrontal cortex during the GNG task compared to rest (Anderson et al., 2014), and increased O_2Hb during 'no-go' trials compared to 'go' trials in lateral prefrontal locations (Herrmann, Plichta, Ehlis, & Fallgatter, 2005). However, these studies simply looked at neural activation between trial types. When actual responses to the GNG task are taken into account, successful behavioral inhibition during 'no-go' trials has been shown to predict lower O_2Hb in the medial prefrontal cortex but not in lateral locations (Rodrigo et al., 2014). Together these findings indicate that increased activation in frontal lateral areas (such as the inferior frontal gyrus) may be associated with the presentation of the 'no-go' condition or behavioral inhibition opportunity itself, but that successful behavioral inhibition appears to specifically be associated with decreased activity in the mPFC. This distinction may account for discrepancies across fMRI studies. Importantly, the NVM posits that the mPFC is integral in the top-down, tonic inhibition of the CAN, and that its role within the network is characterized by heightened activation when resting HFHRV is high. However, during a behavioral inhibition task the relationship between these variables may differ, which highlights the importance of examining this relationship across various contexts.

The first aim of the present study was to replicate fMRI GNG findings using fNIRS. Furthermore, previous fNIRS findings regarding mPFC activation and its relation to GNG performance, in conjunction with the principles of the NVM, make the use of fNIRS a valuable next step in examining the NVM and behavioral inhibition. For this reason, the second aim of this study was to incorporate simultaneous fNIRS and RSA measurement over the course of a

baseline period, as well as during two variations of the GNG task, to assess their relationship as described in the NVM across various contexts. Exploratory analyses were also conducted to examine the relation of these measures to other behaviors implicated in the model (e.g., behavioral and cognitive rigidity). These aims and their related hypotheses are elaborated below.

Aims & Hypotheses

The following aims were addressed in this study by testing the hypotheses outlined below:

Aim 1

Examine prefrontal areas shown to be related to behavioral inhibition across emotional and neutral contexts in previous imaging studies through fNIRS, using a block-design.

Hypothesis #1a: In a block design, global prefrontal O_2Hb will be higher during the emotional GNG block than the simple GNG block, and the simple GNG block will be higher than the baseline block.

Hypothesis #1b: In a block design, O_2Hb concentrations will differ across regions of the PFC during the emotional GNG block compared to the simple GNG block and the baseline block.

Aim 2

Identify neural correlates of RSA at rest and while engaged in behavioral inhibition tasks to further examine the relationships proposed by the NVM.

Hypothesis #2a: RSA and O_2Hb concentrations in areas of the PFC will be positively related at rest.

Hypothesis #2b: RSA and O_2Hb concentration will be related to activation in areas of the PFC during the simple GNG.

Hypothesis #2c: RSA and O_2Hb concentration will be related to activation in areas of the PFC during the emotional GNG.

Exploratory Analyses

Establish how PFC activation, RSA, and performance on a behavioral inhibition task relate to behavioral scales.

Hypothesis #3a: Performance on the simple GNG task will predict cognitive flexibility (as measured by self-report scales).

Hypothesis #3b: PFC activation from areas identified in Aim 2, Hypothesis #2b will predict additional variance in cognitive flexibility (as measured by self-report scales) when controlling for performance.

Hypothesis #3c: Performance on the emotional GNG task will predict cognitive flexibility (as measured by a self-report scale).

Hypothesis #3d: PFC activation from areas identified in Aim 2, Hypothesis #2c will predict additional variance in cognitive flexibility (as measured by a self-report scale) when controlling for performance and social skill ability.

Method

Subjects

Subjects were recruited through the healthy volunteer database at the National Institutes of Health in Bethesda, MD and were compensated for their time participating in the study. The target sample size was 40 subjects ages 18 and above, with an equal number of males and females. This size was based on numbers across many imaging studies examining GNG performance, including both fMRI and fNIRS studies. Exclusionary criteria included: past or present vascular disease, skin disease, or any history of head injury, cardiovascular disease or

congenital heart condition, seizure, or stroke. A total of 43 subjects were brought in to the lab to participate in the study. Subjects were asked to complete a health history questionnaire which screened for psychiatric diagnoses. One subject was excluded from the study due to a psychiatric diagnosis. Furthermore, due to data loss in either the fNIRS or ECG signals, certain analyses contain different samples sizes. A summary of this can be seen in Figure 1.

Demographics. Subjects were 43 healthy adults between the ages of 20 – 66 years old (Males: *M*=35.70; *SD*=14.88; Females: *M*=33.74; *SD*=11.80). Due to data loss, two sets of subjects were used for the subsequent analyses. Demographic data on the first set of subjects used to address Aim 1 are presented in Table 1. Demographic data on the second set of subjects used to address Aim 2 are presented in Table 2.

Measures

Behavioral scales. Subjects were asked to fill out a series of behavioral scales to assess their cognitive and social skills. To examine cognitive flexibility the Cognitive Flexibility Inventory (Dennis & Wal, 2010) was administered. The Cognitive Flexibility Inventory (CFI) is a 20-item self-report questionnaire that assesses the ability to think flexibly and adapt in difficult situations. This self-report measure provided information about subjects' cognitive and behavioral flexibility across a variety of contexts to examine whether this was related to their performance on the cognitive tasks administered in the study.

Subjects also filled out the Autism-Spectrum Quotient (AQ) to assess their social skills. The AQ is a 50-item self-report questionnaire for individuals ages 16 and older (Baron-Cohen, Wheelwright, Skinner, Martin, & Clubley, 2001). The AQ has been shown to provide a range of scores for individuals with an ASD diagnosis as well as those without (Ruzich et al., 2015), thus providing scores for subclinical social deficits. This score was to be used as a covariate for the

emotional GNG task in the exploratory analyses if necessary because the task incorporates social stimuli.

The Edinburgh Handedness Inventory (EDI) was also administered to subjects to assess their handedness (Oldfield, 1971). The EDI provides a laterality score between -100 (left handed) and 100 (right handed). Handedness has been shown to effect lateralization of neural activation, and thus was noted for each subject in the present study.

Electrocardiogram. Electrocardiogram (ECG) was collected through the BioPac MP160 system, outfitted with an ECG amplifier (ECG100C). The ECG100C amplifier records the heart's electrical activity and samples at a rate of 1000 Hz. The MP160/ECG100C hardware was set to an amplifier gain of 1000, low pass filter of 35 Hz and high pass filters of 0.5 Hz and the signal was recorded through AcqKnowledge 4.4 software (BioPac Systems Inc.). A Lead II configuration was used to collect the ECG, which requires that an Ag-AgCl spot electrode be placed underneath the subject's left collar bone on the chest, and underneath the rib cage on their right side. RSA was then derived from this signal through Kubios HRV software using frequency-based (i.e., HFHRV) metrics. Frequency-domain spectral estimates in the high-frequency band (0.12-0.40 Hz) were derived through Fast Fourier Transform. These values were natural log (ln) transformed to correct for their exponential distribution, as is typical in HFHRV analyses (Ellis, Sollers, Edelstein, & Thayer, 2008).

Functional near-infrared spectroscopy. Neural activity was measured through a continuous wave fNIRS device (fNIR Devices LLC), which emits light at two wavelengths (730 nm and 850 nm) and collects at a sampling rate of 2 Hz. The use of two wavelengths of infrared light allows both oxy- and deoxy-hemoglobin levels to be measured, in that they produce differential amounts of backscatter to be picked up by the detectors. The system uses 4 sources

and 10 detectors that are spaced 2.5 cm from another, creating a 16-channel silicone headband that was placed across the forehead of subjects to measure prefrontal activity. Data from the device were collected through COBI Studio software (Ayaz et al., 2011).

Procedure

The protocol for this study was approved by the *Eunice Kennedy Shriver* National Institute of Child Health and Human Development's Institutional Review Board. Subjects were instructed to abstain from alcohol for 24 hours, caffeine for 6 hours, and vigorous exercise for 2 hours prior to their data collection session. All subjects were scheduled for their session to begin between the hours of 8:15 am – 11:30 pm. Upon entering the lab, the subject was provided a copy of the informed consent and reviewed it with the researcher. Once the subject provided consent, they were outfitted with ECG electrodes and a respiration monitor. The ECG and respiration signal were then examined to ensure that the physiological equipment was properly and securely applied. Once this was completed, the subject was asked to fill out the series of behavioral scales. These questionnaires took approximately 15 minutes to complete. After they finished these forms, the fNIRS headband was applied and the signals were checked to ensure that the headband had been properly applied. After this was done, the physiological and neural imaging portion of the session began. Subjects were positioned in front of a computer equipped with E-Prime 2 Stimulus Presentation software (Schneider, Eschman, & Zuccolotto, 2002), which presented all instructions and tasks for the remainder of the data collection session.

Baseline. Subjects first completed the health history questionnaire and behavioral scales, which allowed for adequate time to acclimate to the lab environment. Immediately afterward, a 6:30 minute baseline recording period began. During this, the subject was instructed to sit quietly while watching a mildly stimulating video clip (Coral Sea Dreaming: Plankton Productions &

MJL Network, 2014) presented on a computer monitor, known as a "vanilla" baseline (Jennings, Kamarck, Stewart, Eddy, & Johnson, 1992). A "vanilla" baseline is commonly used in psychophysiological recording as it maintains minimal engagement and creates more uniform conditions across subjects than a traditional baseline. During this time, physiological and neural imaging data was collected.

Cognitive task. Subjects then completed two versions of a GNG task: the simple GNG and the emotional GNG. The order of the tasks was randomized across subjects to control for order effects.

Simple go/no-go. The simple GNG paradigm uses basic stimuli (e.g., numbers, letters, shapes) to examine behavioral inhibition abilities. In the present study, a go/no-go paradigm using letter stimuli was presented to subjects through E-Prime 2. The timing and proportion standards for both the simple GNG and emotional GNG used in this study were modeled after a previous study that used both the simple and emotional GNG task (Schulz et al., 2007). Each block consisted of 192 total trials. These trials were comprised of 75% 'go' stimuli and 25% 'no-go' stimuli (144 'go' and 48 'no-go'). Each stimulus was presented for 500 ms followed by a psuedorandom interstimulus interval (ISI) of 1500 +/- 250 ms. The jitter of the ISI is used to reduce the effect of anticipation of the stimulus on the subject's reaction time. With these timing parameters, the task was approximately 6 minutes and 24 seconds long. When the task began, the following instructions appeared on the screen:

"During this task you will view a series of letters.

When you see the letter 'Y', press the <SPACE> bar.

When you see the letter 'X', do not press any buttons.

Press the <SPACE> bar to continue to the practice trials if you understand these instructions."

The subject was then given six practice trials of the task. Upon completion of these trials, the task began.

Emotional go/no-go. The emotional GNG paradigm follows the same basic rules as the simple go/no-go task; however, neutral versus emotional faces are used as stimuli instead of letters. In this study, neutral faces were the 'go' signal and emotional faces (happy/angry) were the 'no-go' signal. The same timing and proportion parameters were used in the creation of this paradigm as for the simple GNG paradigm described above. The faces used in this version of the task were taken from the Chicago Face Database (Ma, Correll, & Wittenbrink, 2015) and consisted of male and female, Caucasian and African-American models. When the task began, the following instructions appeared on the screen:

"During this task you will view a series of faces.

When you see a face with a neutral expression, press the <SPACE> bar.

When you see a face with an emotional expression, do not press any buttons.

Press the <SPACE> bar to continue to the practice trials if you understand these instructions."

The subject was then given six practice trials of the task. Upon completion of these trials, the task began. Appendix A is a timeline of the simple GNG and the emotional GNG paradigms.

Data Processing

Data processing was conducted on ECG and fNIRS data to remove artifact, normalize values, and calculate the biological metrics of interest. A schematic of the data processing pipeline is depicted in Figure 2.

Pre-processing ECG.

All ECG data were pre-processed using AcqKnowledge 4.4 software for each subject. First, event markers sent from the EPrime script were located in the ECG file and their times

were recorded for later use in calculating the sliding window parameters. Next, the 'Find Cycle' function was used to automatically detect and mark R-spikes in the ECG signal. These marks were then visually inspected to ensure that aberrations in the ECG signal were not mistakenly marked as R-spikes, and that R-spikes were not missed by the algorithm. The 'Find Cycle' function was used again to locate these visually inspected marks and then calculate the time between each R-spike pair (i.e., the interbeat interval) in milliseconds. These values were then saved as a text file which contained two columns: time, and inter-beat interval length (ms).

Pre-processing fNIRS.

The imaging data were pre-processed by subject through fnirSoft Professional v. 4.9 (Ayaz, 2010) to remove motion artifact and physiological noise. First, the event markers sent from the EPrime script in each file were located and their times were recorded for use in the sliding window parameter calculations. Then, the raw light file for each subject was median filtered to remove minor motion artifact, followed by the sliding motion artifact rejection (SMAR) filter to eliminate any sections of data that were still contaminated by excessive motion artifact or over- or under-saturated channels. The light file was then converted into a hemoglobin file through the application of the Modified Beer Lambert Law (MBLL). Depending on the wavelengths of light that are used, the MBLL allows for the calculation of oxygenated and deoxygenated hemoglobin concentration (μm) in a highly scattering medium, such as biological tissues, by accounting for scattering losses and a longer optical path length because of scattering. The hemoglobin file contains the change in the oxygenated hemoglobin (O_2Hb) and deoxygenated hemoglobin (HHb) signals over the course of the data collection period. Linear detrending (first order) was applied to this file to control for signal drift. Finally, a low-pass finite impulse response (FIR) filter (cutoff: 0.1 Hz; order: 20) was applied to the signal to reduce

physiological noise introduced to the signal from sources such as heart beat and respiration (Huppert, Diamond, Franceschini, & Boas, 2009). The time, O_2Hb, and HHb values were then saved as text files for each subject. Finally, the O_2Hb time series for each subject was z-scored by channel.

Post-processing ECG & fNIRS.

For each subject, the event markers from their ECG data file and their fNIRS data file were used to calculate the parameters for their sliding window epochs to be used for subsequent analyses. The window length was set to 30 seconds with 7 seconds of overlap with adjacent windows, resulting in 46.67% overlap between adjacent windows. For each condition this resulted in 16 windows, for a total of a 6:15 minute condition period. This was done to generate start and stop times for each window within each condition for both the ECG and fNIRS signals. The window values from the ECG signal were then used to compute RSA (e.g., lnHFHRV) for each 30 second window (Takahashi, Kuriyama, Kanazawa, Takahashi, & Nakayama, 2017) in Kubios HRV software from the IBI files previously mentioned. The window values from the fNIRS signal were then used to compute the mean of the standardized O_2Hb signal within each window for each channel. The corresponding RSA and O_2Hb values were then used to complete subsequent analyses for each subject.

Analyses

The following analyses were conducted to assess the hypotheses of the present study.

Aim 1: Examine prefrontal areas shown to be related to behavioral inhibition across emotional and neutral contexts in previous imaging studies through fNIRS using a block-design.

Hypothesis #1a: In a block design, global prefrontal O_2Hb will be higher during the emotional GNG block than the simple GNG condition, and the simple GNG condition will be higher than the baseline condition.

Hypothesis #1b: In a block design, O_2Hb concentrations will differ across regions of the PFC during the emotional GNG condition compared to the simple GNG condition and the baseline condition.

Standardized O_2Hb values (by channel within each subject) were used as the dependent variable to evaluate whether neural activation varied across the conditions. Due to signal loss, a repeated measures ANOVA could not be used to address these hypotheses. Instead, a linear mixed effects model with 'condition' and 'channel' as fixed effects and 'subject' as a random effect was used. Hypothesis #1a was evaluated by seeing whether the main effect of 'condition' was significant (and the interaction between 'condition' and 'channel' remained ordinal). Hypothesis #1b was evaluated by seeing whether the interaction between 'condition' and 'channel' was significant.

Aim 2: Identify neural correlates of RSA at rest and while engaged in behavioral inhibition tasks in service of further examining the relationships proposed by the NVM.

Hypothesis #2a: RSA and O_2Hb concentrations across areas of the mPFC will be positively related at baseline.

RSA (lnHFHRV) and O_2Hb concentrations were quantified over the baseline period through a sliding window analysis. Doing this allowed a series of RSA and O_2Hb values to be generated at multiple time points over the baseline period so that the correspondence between these values could be tracked over the baseline time course for each subject. These analyses were modeled after those conducted by Chang et al. (2013), who performed similar analyses to compare lnHFHRV and fMRI signals. These values were entered in a subject-level general linear model

(GLM) to determine whether RSA predicted O_2Hb concentration. This was done for each subject at each channel, providing 16 channel parameter estimates per subject per condition to be used for statistical analyses in subsequent steps.

$$\widehat{Y_n} = \beta_0 + \beta_1 X_n$$

Where… $\hat{Y}$= O_2Hb concentration time series for channel *j*

j = fNIRS channel number

X = RSA time series

β_0 = y-intercept

β_1 = slope for RSA on O_2Hb

n = subject

Running these models for each channel for each subject yielded a *n* (subject) by 16 (fNIRS channels) matrix of standardized parameter estimates (β). Again, due to missing data, a repeated measures ANOVA could not be used to evaluate this hypothesis. Instead, a linear mixed effects model was used to evaluate if there was a significant fixed effect of 'channel' with 'subject' modeled as a random effect on the standardized parameter estimates (β) during baseline. If the model was significant, this would indicate that the relationship between RSA and activation of at least one channel was different than the rest of the PFC and supports the hypothesis that activation at a specific region of the prefrontal cortex was related to RSA. Planned contrasts using all pairwise comparisons were then performed using the Holm-Bonferroni method of sequentially rejective t-tests (Holm, 1979) to determine which channels had significantly different relationships with RSA from each another. Hypothesis #2a would be further supported if medial channels (channels 7-10) were shown to have significantly larger relationships with RSA.

Hypothesis #2b: RSA and O_2Hb concentration will be related in areas of the PFC during the simple GNG.

The same approach described for Hypothesis #2a was used to assess Hypothesis #2b, except that the parameter estimates (β) were calculated using the time series data from the simple GNG task. Hypothesis #2b would be supported if a mixed effects model shows a significant main effect of channel. Planned contrasts using all pairwise comparisons were then performed using the Holm-Bonferroni method to determine which channels had significantly different relationships with RSA from each another. Channels that were revealed to have significantly different parameter estimates were to be used in the analyses to evaluate Hypothesis #3b.

Hypothesis #2c: RSA and O_2Hb concentration will be related with activation in areas of the PFC during the emotional GNG.

The same approach described for Hypothesis #2a was used to assess Hypothesis #2c, except that the parameter estimates (β) were calculated using the time series data from emotional GNG task. Hypothesis #2c would be supported if a mixed effects model examining differences in the relationship between RSA and O_2Hb (β) across the fNIRS channels showed a significant main effect of channel. Planned contrasts using all pairwise comparisons were then performed using the Holm-Bonferroni method to determine which channels had significantly different relationships with RSA from each another. Channels that were revealed to have significant parameter estimates were to be used in the analyses to evaluate Hypothesis #3c.

Exploratory Analyses: Establish how PFC activation, RSA, and performance on a behavioral inhibition task relate to behavioral scales.

Hypothesis #3a: Performance on the simple GNG task will predict cognitive flexibility (as measured by self-report scales).

Accuracy (% correct) for the simple GNG task was calculated and used as a predictor for scores on the Cognitive Flexibility Inventory ($\hat{Y}$).

$$\hat{Y} = \beta_0 + \beta_1 X_1$$

Where… $\hat{Y}$ = Cognitive Flexibility Inventory (CFI) score

β_0 = y-intercept

β_1 = slope for $\text{accuracy}_{\text{simple}}$ on CFI score

X_1 = $\text{accuracy}_{\text{simple}}$

If the regression coefficient was significant, this would support the hypothesis that performance on the simple GNG predicts cognitive flexibility.

Hypothesis #3b: PFC activation from areas identified in Aim 2, Hypothesis #2b will predict additional variance in cognitive flexibility (as measured by self-report scales) when controlling for performance.

If the regression model in Hypothesis #3a was found to be significant, the mean concentration of O_2Hb at the channels identified as having an increased PFC x RSA relationship in Hypothesis #2b was to be added as a predictor to the regression model from Hypothesis #3a, resulting in the following model:

$$\hat{Y} = \beta_0 + \beta_1 X_1 + \beta_2 X_2$$

Where… $\hat{Y}$ = CFI score

β_0 = y-intercept

β_1 = slope for $\text{accuracy}_{\text{simple}}$ on CFI score

X_1 = $\text{accuracy}_{\text{simple}}$

β_2 = slope for O_2Hb_{simple} on CFI score

X_2 = O_2Hb_{simple}

If the regression coefficient β_2 was significant, this would support the hypothesis that PFC activation predicts additional variance in cognitive flexibility.

Hypothesis #3c: Performance on the emotional GNG task will predict variance in cognitive flexibility (as measured by a self-report scale).

Accuracy (% correct) for the emotional GNG task was calculated and used as a predictor variable for scores on the Cognitive Flexibility Inventory ($\hat{Y}$).

$$\hat{Y} = \beta_0 + \beta_1 X_1$$

Where… $\hat{Y}$ = Cognitive Flexibility Inventory score

β_0 = y-intercept

β_1 = slope for $\text{accuracy}_{\text{emotional}}$ on CFI score

X_1 = $\text{accuracy}_{\text{emotional}}$

If the regression coefficient β was significant, this would support the hypothesis that emotional GNG performance predicts variance in cognitive flexibility.

Hypothesis #3d: PFC activation from areas identified in Aim 2, Hypothesis #2c will predict additional variance in cognitive flexibility (as measured by a self-report scale) when controlling for performance and social skill ability.

Building on the regression model in Hypothesis #3c, the mean O_2Hb in areas of heightened PFC activation identified in Aim 2, Hypothesis #2c would be added as a predictor to the regression model, resulting in the following model:

$$\hat{Y} = \beta_0 + \beta_1 X_1 + \beta_2 X_2 + \beta_3 X_3$$

Where… $\hat{Y}$ = CFI score

β_0 = y-intercept

β_1 = slope for $\text{accuracy}_{\text{emotional}}$ on CFI score

X_1 = $accuracy_{emotional}$

β_2 = slope for Autism Spectrum Quotient score on CFI score

X_2 = Autism Spectrum Quotient score

β_3 = slope for $O_2Hb_{emotional}$ on CFI score

X_3 = $O_2Hb_{emotional}$

If the regression coefficient β_3 was significant, this supports the hypothesis that PFC activation during the emotional GNG predicts additional variance in cognitive flexibility.

Results

Behavioral Performance

Behavioral performance on the Simple GNG and Emotional GNG was compared to examine whether the Emotional GNG was more challenging, as has been previously shown in the literature (Schulz et al., 2007). A non-parametric paired samples t-test found a significant effect of task (Z=-4.76, p<0.001) such that accuracy (% correct) on the Simple GNG was higher (*Mdn*=0.98; *SD*=0.027) than performance on the Emotional GNG (*Mdn*= 0.89; *SD*=0.075). Furthermore, the reaction time for correct trials was shorter for the Simple GNG (*Mdn*= 434.35; *SD*= 60.93) than the Emotional GNG (*Mdn*=704.00; *SD*= 143.28), (Z=-4.78, p<0.001). These results indicate that the Emotional GNG was more challenging than the Simple GNG, which is congruent with the literature.

Task performance was also examined for a practice effect to see if subjects' performance on either task improved over time. The trials for each task were split in half so that accuracy (% correct) on the first half of trials could be compared to the second half of trials. Nonparametric paired samples t-tests did not indicate performance differences between the first and second half

of trials on the Simple GNG (Z=-.83, p=0.408) or the Emotional GNG (Z=-.10, p=0.918). These results indicate that subjects performed similarly across the length of both tasks and did not improve over time. Similar analyses were conducted to assess whether activation at each channel changed over the course of each task. A nonparametric paired samples t-test was run comparing mean O_2Hb from the first half of the task to mean O_2Hb for the second half of the task at each channel in the Simple GNG condition and the Emotional GNG condition. Due to the large number of contrasts for each condition, these tests were assessed using a Bonferroni correction for 16 contrasts (p< 0.003125). None of the tests indicated differences between the first and second half of the tasks at this level (see the Supplementary Analyses in Appendix B; Table 6 and Table 7).

Aim 1

The remaining statistical analyses were performed in the language and programming environment *R* (R Core Team, 2017). Linear mixed models were conducted through the 'lme4' (Bates, Maechler, Bolker, & Walker, 2015) and 'lmerTest' (Kuznetsova, Brockhoff, & Christensen, 2017) packages and fNIRS activation maps were created using the 'gplots' package (Warnes et al., 2016).

A linear mixed effect model with 'subject' as a random effect, and 'condition' and 'channel' as fixed effects was run using standardized O_2Hb means as the dependent variable. Dummy coding was used for the effect of 'condition', with the baseline condition as the referent cell. Deviation coding was used for the effect of 'channel', thus the beta estimates of the model are relative to the grand mean of all channels.

The analyses did not show an interactive effect between 'channel' and 'condition' (p=0.652025) or a main effect of 'channel' (p=0.999529); however, a main effect of 'condition'

was present (F(2, 1236.6)=5.1732, p=0.005789). Follow-up contrasts revealed that O_2Hb during the Simple GNG task was higher than during baseline (t(1232)=2.915, p=0.00362) and that O_2Hb during the Emotional GNG task was higher than during baseline (t(1232)=2.546, p= 0.01101). There was no difference between the Simple GNG and Emotional GNG task (p=.13605). The activation patterns within each condition are displayed by channel in the O_2Hb activation maps in Figure 3.

Aim 2

A linear mixed effect model with 'subject' as a random effect and 'channel' as a fixed effect was run using the standardized β weights from the subject-level GLMs where RSA predicted O_2Hb during the baseline condition as the dependent variable. Deviation coding was used to define the contrasts in the model, as this coding scheme allows for all channels to be compared to the grand mean. The contrast codes were formulated through the *contrasts* function in R. The omnibus test for this model was not significant, (F(15, 340.93)=1.3504, p=0.1701), indicating that the amount of variance in neural activity predicted by RSA did not vary by channel during baseline. However, since contrasts were determined a priori, differences at the channel level were further examined. At p<0.05, increased RSA predicted lower O_2Hb levels at channel 4 during baseline compared to the grand means of all other channels (β=-0.065, t(341.22)=-2.279, p=0.023) and increased RSA predicted higher O_2Hb levels at channel 12 during baseline compared to the grand means of all other channels (β=0.12, t(342.15)=2.828, p=0.0050). The resulting t-scores from all contrasts for the baseline condition are summarized in Figure 4A. These results were not significant when corrected for the number of comparisons through the Holm-Bonferroni method of sequentially rejective t-tests. A summary of these contrasts is presented in Table 3.

To address Hypothesis #2b, a linear mixed effect model with 'subject' as a random effect and 'channel' as a fixed effect was run using the standardized β weights from the subject-level GLMs where RSA predicted O_2Hb during the Simple GNG condition as the dependent variable. The omnibus test of this model was not significant, (F(15, 325.51)=1.6782, p=0.05375) indicating that the amount of variance in neural activity predicted by RSA did not vary by channel during the Simple GNG. Again, the planned contrasts for this hypothesis allowed for further examination of differences at the channel level. At p<0.05, increased RSA predicted heightened O_2Hb at channel 9 during the Simple GNG (β=0.091, t(325.4)=3.245, p=0.00129). This contrast met significance when using the Holm-Bonferroni method of sequentially rejective t-tests to correct for the number of contrasts, which set the first significance value for the ranked contrasts in this analysis to 0.003125. A summary of these contrasts is presented in Table 4.

To address Hypothesis #2c, a linear mixed effect model with 'subject' as a random effect and 'channel' as a fixed effect was run using the standardized β weights from the subject-level GLMs where RSA predicted O_2Hb during the Emotional GNG condition as the dependent variable. The omnibus test of this model was not significant, (F(15, 266.48)=0.4909, p=0.9443) indicating that the amount of variance in neural activity predicted by RSA did not vary by channel during the Emotional GNG. Furthermore, the planned contrasts for this hypothesis did not reveal differences between channels in the predictive relationship between RSA and O_2Hb during the Emotional GNG. A summary of these contrasts is presented in Table 5.

Exploratory Analyses

The first exploratory analysis examined whether performance on the Simple GNG could predict variance on subjects' scores on the Cognitive Flexibility Inventory. A linear regression using Simple GNG accuracy (% correct) as a predictor was not significant (p=0.9274), indicating

that Simple GNG accuracy does not explain variance in CFI scores. For this reason, the specific proposed analyses to assess Hypothesis #3b were not conducted.

The next exploratory analysis examined whether performance on the Emotional GNG predicted variance in CFI scores. A linear regression using Emotional GNG accuracy (% correct) found that this score predicted CFI scores ($F(1, 26)=6.564$, $p=0.01655$). The adjusted R^2 indicated that accuracy on the Emotional GNG accounted for 20.16% of the variance in CFI scores. However, the analyses examining how well RSA predicted O_2Hb during the Emotional GNG conducted to address Hypothesis #2c did not reveal a predictive relationship at any particular channel during this condition. For this reason, the proposed analysis for Hypothesis #3d was not conducted.

Discussion

The present study found that the level of prefrontal activation as measured by the level of oxygenated hemoglobin (O_2Hb) in the prefrontal cortex was different during behavior inhibition tasks compared to baseline. This was shown in a simple version of the task, as well as in a more complicated version of the same behavior inhibition task. A main effect of condition, such that the Simple GNG and Emotional GNG both caused elevated O_2Hb compared to baseline, supported the hypothesis that increased prefrontal activation would be elicited by the behavior inhibition tasks. However, there was no difference in the level of activation between the two behavior inhibition tasks. Furthermore, when patterns of activation across the prefrontal cortex were examined, hypothesis #1b was not supported, as there was no significant interaction between condition and channel. In part, it appears this was due to widespread prefrontal activation present within both tasks. These findings indicate that while both forms of the task elicit significant prefrontal activation that can be measured through fNIRS, the level is

comparable regardless of task difficulty. These findings are somewhat consistent with the behavioral literature, which suggests that the two different forms of the GNG indicate the same construct (Schulz et al., 2007) and thus would elicit similar activation patterns. Although these findings suggest similar processing across the simple and emotional form of the GNG, it is possible that the differences in neural recruitment are present in other areas of the cortex that were not measured in the present study, or in subcortical areas that cannot be measured using fNIRS. Regardless, these results corroborate previous neural imaging from the fMRI literature, providing evidence that the assessment of neural activation associated with behavior inhibition can be measured through fNIRS. This is particularly valuable for several reasons, including the increased ecological validity, heighted levels of compliance, and reduced concern with motion artifact in fNIRS measurement compared to fMRI. By establishing the feasibility of using fNIRS in assessing neural activation during a behavior inhibition task, this study provides justification for using this more patient-friendly technology to assess future research questions related to neural activity during such tasks.

The results of this study also support the hypothesis that RSA can predict prefrontal activation at rest and during a behavioral inhibition task, which is consistent with the NVM. Though it should be noted that some of these findings were not maintained when corrected for multiple comparisons, the relationship between RSA and prefrontal activation across different conditions in this study was consistent with findings from previous studies examining the NVM. For example, standardized beta weights above the grand mean of other channels during baseline at channel 12 (at the p=0.05 level) reflects a stronger predictive relationship between RSA and right mPFC activation, which is one of the CAN structures implicated in the NVM and is consistent with the previous imaging literature examining the NVM (Thayer et al., 2012). This is

also consistent with the general GNG imaging literature which indicates a dominance of the right hemisphere during this behavior inhibition task (Swick et al., 2011).

Furthermore, this is the first study to examine whether the NVM holds across multiple contexts. Previous studies looking at RSA and neural activation have largely been conducted at rest. Though a few have looked at RSA and neural activation concurrently during a task (e.g., the n-back task, a speech stressor, a handgrip task, a working memory task) none have used a task involving behavior inhibition or cognitive flexibility (Thayer et al., 2012). The present study used a task that is relevant to the cognitions and behaviors implicated in the NVM to determine whether the activity of the CAN (i.e., prefrontal activation) was still indexed by RSA in this context. The predictive relationship of RSA on mPFC activation during the Simple GNG (channel 9, after Bonferroni correction) supported the hypothesis that the NVM would hold during a task involving the recruitment of these neural structures. This has implications for how behavior inhibition and flexibility can be assessed through different biological measures, with the potential for these metrics to be used in the assessment and tracking of inhibition and flexibility deficits.

The study also attempted to delineate a relationship between the measure of behavioral inhibition used in the study (i.e., the GNG task) to a more generalized measure of cognitive flexibility (i.e., the CFI) to see whether the NVM could be applied to additional aspects of everyday functioning that are influenced by this ability. Unfortunately, the exploratory hypotheses proposed in the present study were not supported by the proposed analyses. The null findings could be due in part to a lack of variability in the behavioral performance and cognitive flexibility scores of the sample examined in the present study. For instance, the first set of exploratory analyses did not find that Simple GNG performance predicted CFI scores; however,

this could have been because there was little variability in the Simple GNG scores due to a pronounced ceiling effect. When a more challenging version of the task was used (i.e., the Emotional GNG), performance did predict subjects' CFI scores. Unfortunately, during the Emotional GNG condition, no significant predictive relationship between RSA and any specific prefrontal location was present. For this reason, analyses examining activation during the Emotional GNG in relation to the CFI were not conducted. The extant literature has found that variations of the GNG task show differential neural activation, with more complex versions (e.g., the Emotional GNG, multiple no-go cues) showing activation that was associated with the working memory load of the task, as opposed to the behavioral inhibition demands (Simmonds et al., 2008). These activation differences can occur in areas beyond the PFC, such as the pre-SMA (Criaud & Boulinguez, 2013). The Emotional GNG used in the present study may have been recruiting structures involved in other processes, such as working memory, due to the complexity of the stimuli. This may account for the lack of PFC activity associated with RSA during that condition. The inclusion of a more challenging version of the Simple GNG (e.g., shorter ISIs, more letters) that does not incorporate such complex, valenced stimuli such as the emotional faces used in the Emotional GNG could address this gap in future studies.

The present study replicated previous findings from the fMRI literature using fNIRS to examine prefrontal activation in response to a behavior inhibition task. Increased PFC activation during both the Simple GNG and Emotional GNG in relation to baseline indicated global PFC recruitment during these tasks. Although differences in the level of activation or pattern of activation between the two tasks were not detected in the present sample, the study provides support for using fNIRS to investigate behavior inhibition tasks and potential differences between the variations in these tasks in future studies. Furthermore, the study added to the

current neuroimaging literature examining the NVM by implementing a different neuroimaging approach (i.e., fNIRS, simultaneous RSA and neural assessment) and the incorporation of relevant task-based measures in addition to resting state measurement.

Limitations

Although the present study improves upon the current state of the neural imaging literature surrounding the NVM, there are a few limitations that will require replication to validate the findings. First, the sample size for Aim 2 of the study was approximately 33 subjects. Though 43 subjects were brought in to the lab to participate, there was data loss for several reasons, such as fNIRS signal loss, ECG signal loss, and issues with understanding task direction. Of the three primary fMRI studies that have examined RSA and neural activation in a similar manner, this sample size is comparable (Chang et al., 2013) (N=35) if not larger (Napadow et al., 2008) (N=7), (Critchley et al., 2003)(N=6). Since the present study was the first to use fNIRS to address this research question, the proposed sample size estimate was based on the fMRI literature. A sample size on the larger end of previously conducted work was chosen, as fMRI generally has a greater signal-to-noise ratio than fNIRS (Cui, Bray, Bryant, Glover, & Reiss, 2011). However, many of the analyses did not reach statistical significance when using the Holm-Bonferroni correction for multiple comparisons, though they did at the level of p=0.05 and were consistent with findings from previous studies. These results indicate that increasing the sample size in future replications of the present study is warranted.

Lastly, the analyses in the present study were largely based on previous fMRI studies that have examined the NVM through traditional fMRI analysis procedures (Chang et al., 2013). While these methods are standard in the field, recent work suggests that there are more advanced statistical approaches that can be applied to imaging data. A majority of the fMRI literature

utilizes a summary statistic approach, wherein subject-level regressions are conducted at the voxel level and the summary statistics (i.e., β estimates) resulting from these analyses are used to conduct group-level analyses (Monti, 2011). The issue with this approach is that it does not account for individual variances from the subject-level equations when conducting group-level analyses. More recently, fMRI researchers have been advocating for the use more comprehensive statistical approaches, such as the "sufficient-summary-statistic approach" (Dowding & Haufe, 2018), or the use of hierarchical/multi-level linear models (Chen, Saad, Britton, Pine, & Cox, 2013) when analyzing neuroimaging data. These approaches allow nested data to be modeled, accounting for potential individual differences in variance, which leads to more accurate and robust statistical models. In the present study, the analyses were intentionally modeled after previous fMRI research because multiple hypotheses and corresponding research design elements were already being newly introduced (e.g., the use of fNIRS, adding multiple conditions to examine research questions examining the NVM). However, these more robust modeling approaches should be considered when examining these research questions moving forward.

Future Directions

In addition to the more advanced statistical modeling approaches mentioned above, several other approaches should be employed, and research questions pursued in relation to the findings from this study. First, PFC activation in relation to RSA should be assessed across additional cognitive tasks related to behavioral inhibition and cognitive flexibility. For example, in addition to replicating the present study with more complex versions of the Simple GNG task, various versions of the Stroop Color-Word task could be used to examine inhibition of cognitive interference (Scarpina & Tagini, 2017) and other task-switching or set shifting paradigms

(Dajani & Uddin, 2015). Assessing the relationship between PFC activation and RSA across various aspects of cognitive flexibility in this way will help validate whether the biological principles behind the NVM generalize across contexts or could reveal whether these metrics differentially relate to various components of cognitive flexibility. These findings could have important implications for how these biological metrics could be utilized for individuals with deficits in cognitive flexibility.

Second, as mentioned previously, the principles of the NVM in conjunction with these neuroimaging results could have important implications for the potential use of these biological metrics as indicators of deficits in cognitive and behavioral flexibility. To determine whether this will be feasible, research investigating whether there is a relationship between these metrics and more general cognitive and behavioral flexibility deficits must be conducted. Although there is evidence of this in the literature, no previous study has simultaneously looked at PFC activation, RSA, and these deficits. Although this was attempted in the present study, a lack of variability within the samples' performance and flexibility measures limited the ability to detect a meaningful effect. In order to thoroughly bridge the gap between the biological metrics and deficits in cognitive and behavioral flexibility a number of approaches can be incorporated into future studies. First, thorough behavioral phenotyping of subjects beyond the use of self-report scales, such as the CFI, will need to be performed in order to understand the variability in functioning across subjects. Second, recruitment of subjects should encompass a wide array of abilities within the flexibility domain, which could be achieved through the incorporation of clinical populations affected by deficits in this area. Third, studies that manipulate either the biological or behavioral components related to the NVM should be conducted. Behavioral treatment approaches focused on increasing cognitive or behavioral flexibility should be done

while using the biological metrics associated with the NVM as additional outcome variables. If increases in cognitive and behavioral flexibility are behaviorally evident along with changes in these biological metrics, this would provide strong evidence for the use of either PFC activation or RSA as a biomarker of these functions. Conversely, a biofeedback approach focused on altering RSA in conjunction with PFC measures and behavioral measures as additional outcome variables would offer similar insight. Together such research would have important implications in the treatment and assessment of deficits in cognitive and behavioral flexibility.

Conclusion

The present study examined prefrontal activation during two forms of a behavioral inhibition task through fNIRS, used simultaneous assessment of neural and parasympathetic output to improve upon prior evaluations of the NVM, and attempted to relate task performance, neuroimaging, and RSA measures during behavioral inhibition to deficits in other areas related to behavioral and cognitive flexibility. The findings from the present study not only elucidate theoretical questions about the NVM, but also speak to broader applications of the model to other domains of functioning. From a methodological perspective, the present study provides valuable information regarding the use of fNIRS in conjunction with RSA to evaluate the NVM. The findings using fNIRS are consistent with previous studies that have used fMRI to investigate research questions surrounding the model and behavior inhibition. The present study indicates that fNIRS is a viable alternative to fMRI, which is comparatively more cumbersome and expensive, in assessing these research questions. From a theoretical perspective, the present study provides information about the NVM beyond the previous literature through assessment at baseline as well as during behavior inhibition. Specifically, the findings indicate that the relationship between RSA and prefrontal activation proposed in the model is likely to vary

depending on environmental demands. These findings indicate the importance of assessing the NVM across multiple contexts moving forward and, consequently, provide insight for how these measures may be applied in addressing behavioral flexibility deficits. Incorporating these considerations into future studies will be imperative in assessing the practicability of using the biological markers proposed in the NVM as potential therapeutic targets or evaluation tools for these deficits.

Figure 1. Flowchart of subject sample sizes.

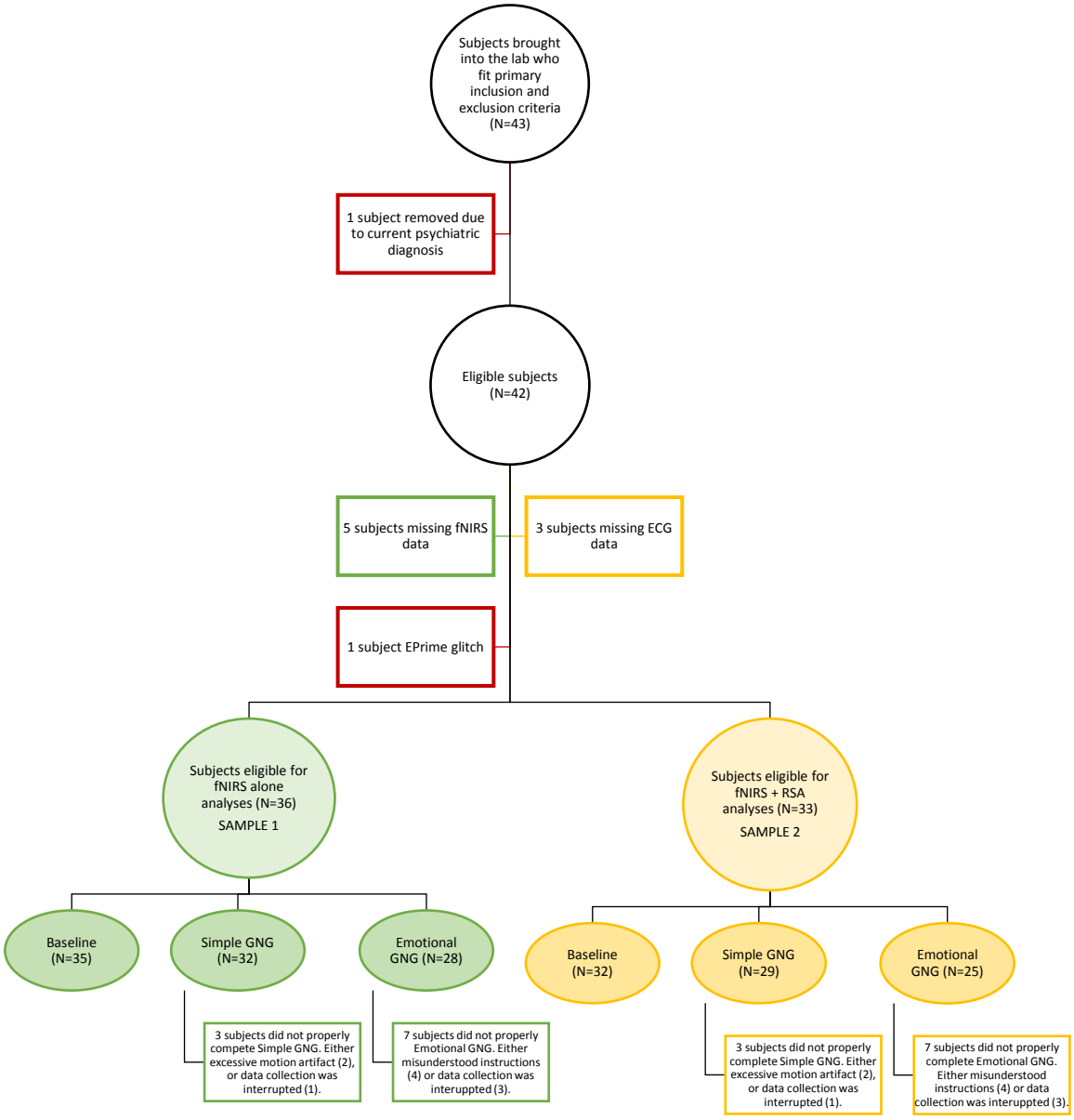

Figure 2. Data processing pipeline.

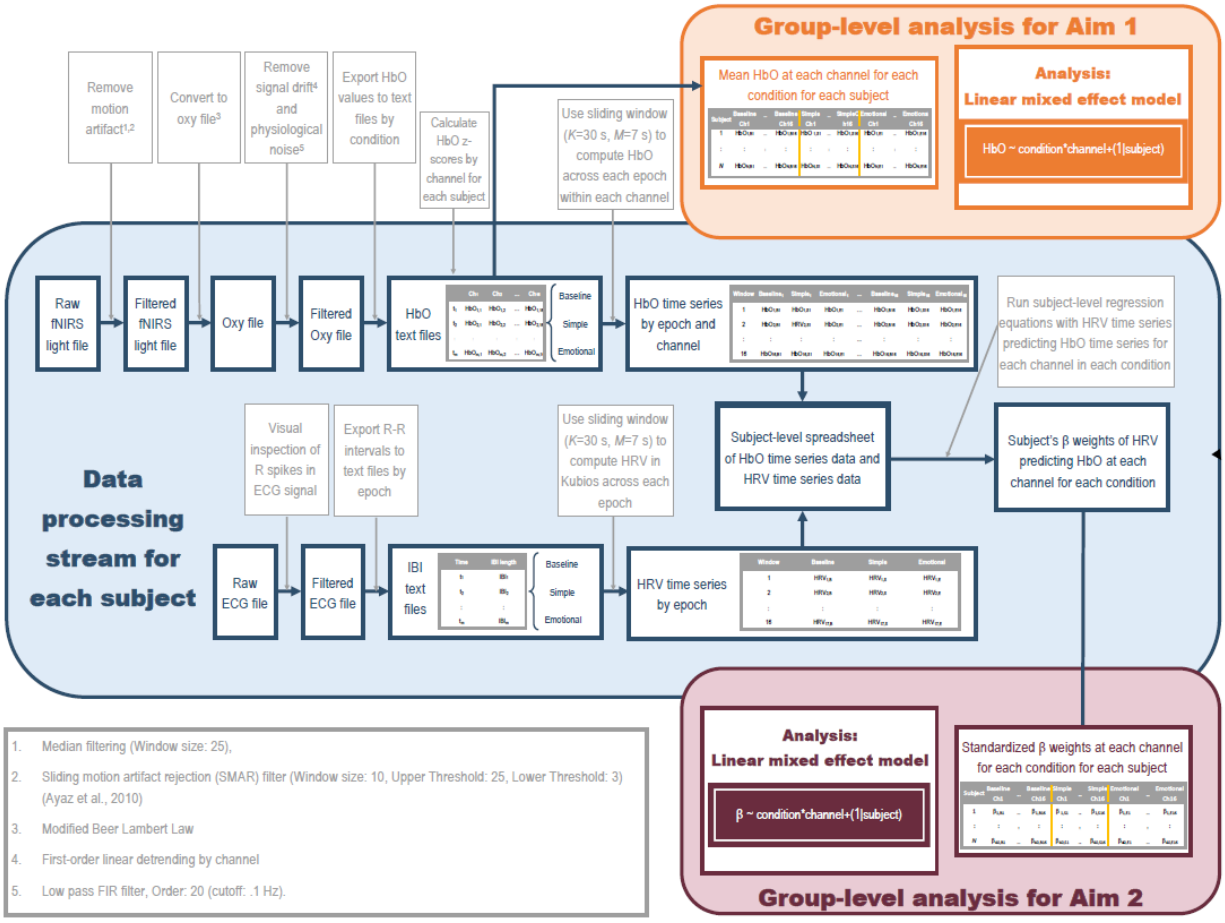

Figure 3. O_2Hb activation maps across Baseline, Simple GNG, and Emotional GNG.

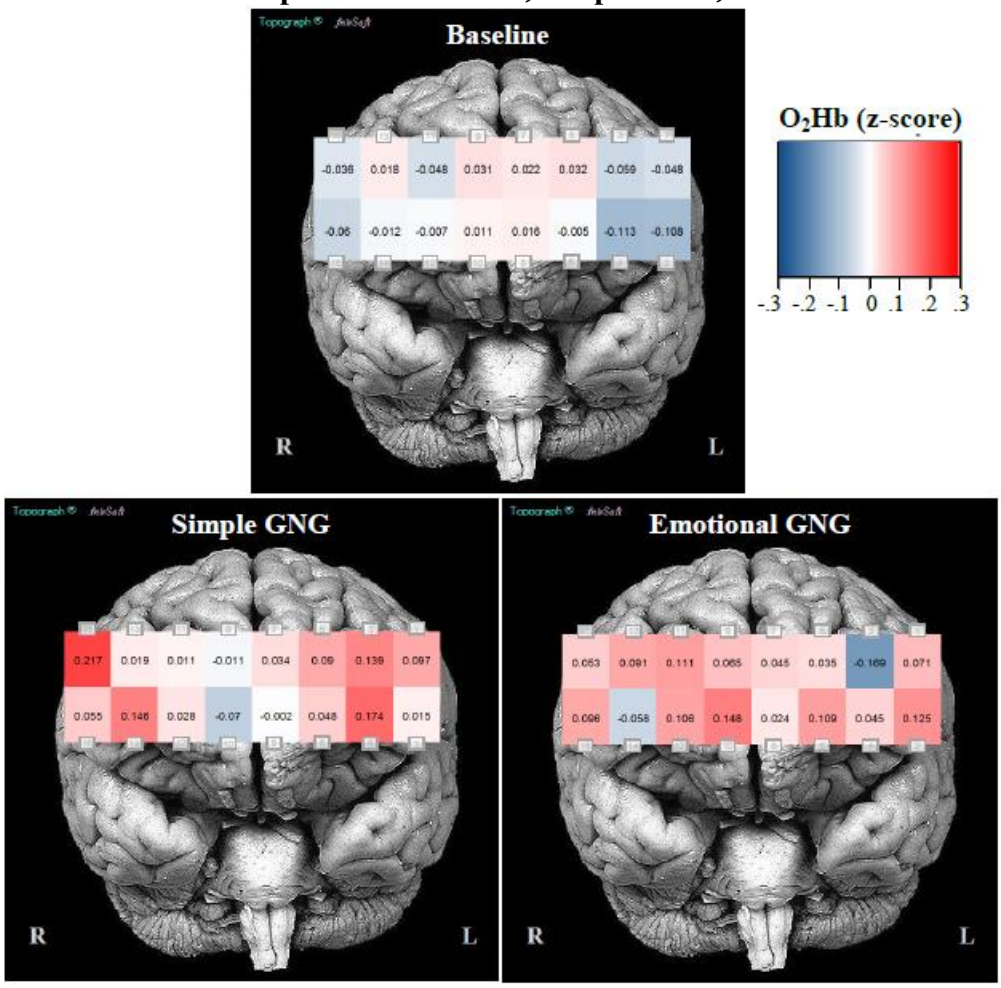

Figure 4. Results of the linear mixed model standardized β estimates by channel compared to the grand mean of standardized β estimates within each condition.

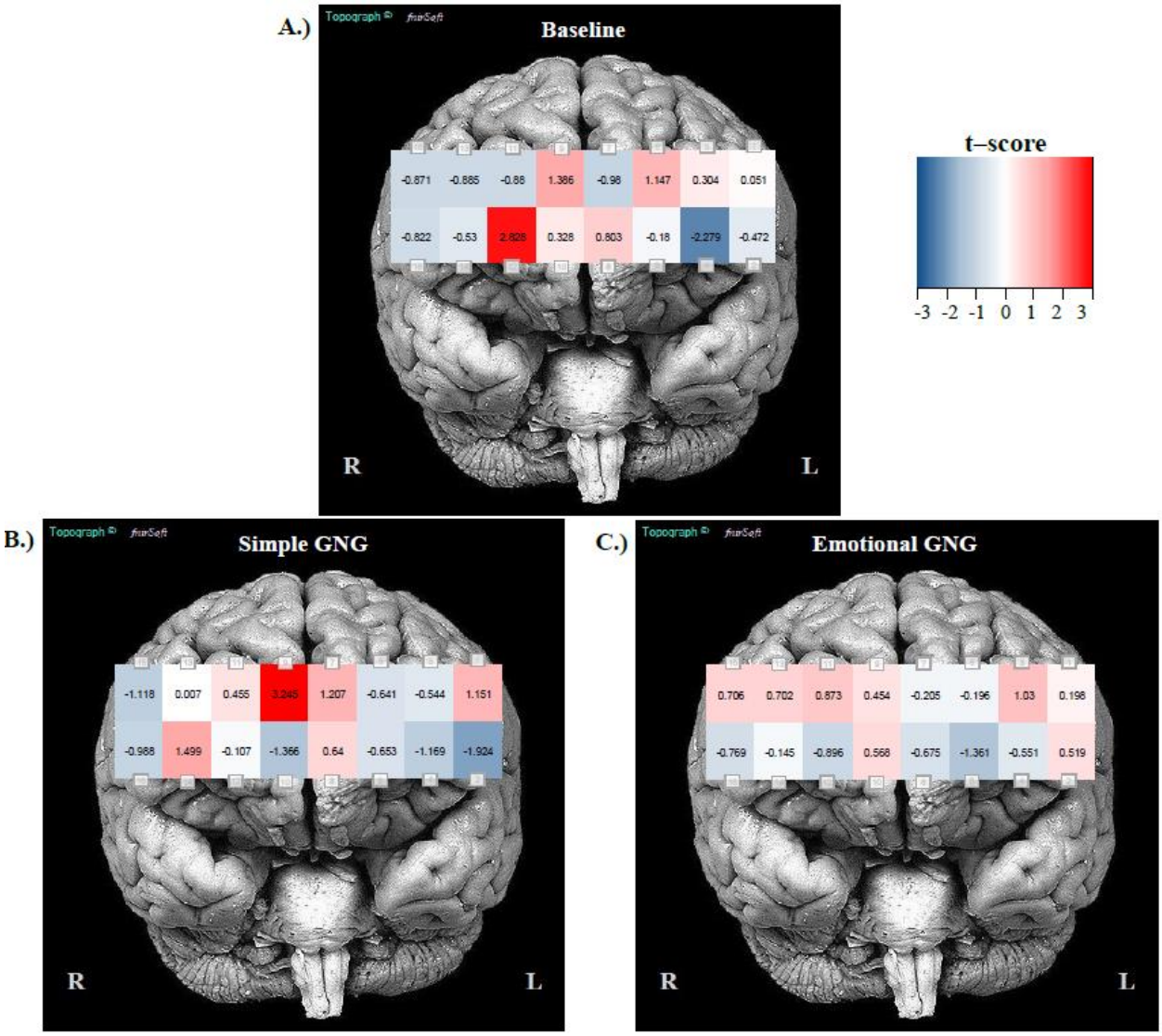

Table 1. Demographics for Sample 1 (*n*=36).

	Mean	***SD***	***Min***	***Max***
Age (years)	34.64	12.81	20.00	66.00
Body Mass Index (BMI)	26.52	5.57	19.00	44.80
Cognitive Flexibility Inventory	116.56	14.28	82.00	140.00
Simple GNG (% correct)*	0.97	0.03	0.89	1.00
Emotional GNG (% correct)^	0.88	0.08	0.61	0.97
Sex (M : F)	15.00		21.00	
EDI Handedness (L : A : R)@	3.00	3.00	29.00	

Note. GNG = Go/No-Go; EDI = Edinburgh Handedness Inventory; L = left-handed; A = ambidextrous; R = right-handed.

* 1 subject spoke during task; 1 had excessive motion artifact. Excluded from these averages.

^ 2 subjects spoke during task; 3 subjects misunderstood directions. Excluded from these averages.

@ 1 subject did not properly fill out the EDI.

Table 2. Demographics for Sample 2 (*n*=33).

	Mean	***SD***	***Min***	***Max***
Age (years)	35.64	12.93	20.00	66.00
Body Mass Index (BMI)	26.45	5.34	19.00	44.80
Cognitive Flexibility Inventory	116.33	14.69	82.00	140.00
Simple GNG (% correct) *	0.97	0.03	0.89	1.00
Emotional GNG (% correct) ^	0.88	0.06	0.73	0.97
Sex (M : F)	14.00		19.00	
EDI Handedness (L : A : R) @	2.00	3.00	27.00	

Note. GNG = Go/No-Go; EDI = Edinburgh Handedness Inventory; L = left-handed; A = ambidextrous; R = right-handed.

* 1 subject spoke during task; 1 had excessive motion artifact. Excluded from these averages.

^ 2 subjects spoke during task; 3 subjects misunderstood directions. Excluded from these averages.

@ 1 subject did not properly fill out the EDI.

Table 3. Summary of the linear mixed model examining whether channel activation was differentially predicted by RSA (standardized β) for Baseline.

Channel number	***β* estimate**	***SE***	***df***	***t***	***p***
(Intercept)	-0.074	0.036	32.043	-2.038	0.050
1	0.002	0.033	341.183	0.051	0.959
2	-0.013	0.028	340.495	-0.472	0.637
3	0.009	0.030	340.767	0.304	0.761
4	-0.065	0.028	340.404	-2.279	0.023*
5	0.039	0.034	341.222	1.147	0.252
6	-0.006	0.033	341.007	-0.180	0.857
7	-0.035	0.035	341.383	-0.980	0.328
8	0.024	0.030	340.607	0.803	0.423
9	0.041	0.030	340.777	1.386	0.167
10	0.010	0.032	340.842	0.328	0.743
11	-0.027	0.030	340.821	-0.880	0.380
12	0.117	0.041	342.153	2.828	0.005*
13	-0.029	0.032	341.040	-0.885	0.377
14	-0.017	0.032	340.976	-0.530	0.597
15	-0.027	0.031	340.981	-0.871	0.384
16	-0.024	0.029	340.641	-0.822	0.412

Note. Deviation coding was used in this model. All β estimates relative to the grand mean. *p<0.05, two-tailed. **p<0.01, two-tailed.

Table 4. Summary of the linear mixed model examining whether channel activation was differentially predicted by RSA (standardized β) for the Simple GNG.

Channel number	***β* estimate**	***SE***	***df***	***t***	***p***
(Intercept)	-0.014	0.042	30.130	-0.324	0.748
1	0.035	0.031	325.600	1.151	0.251
2	-0.051	0.027	325.300	-1.924	0.055
3	-0.016	0.029	325.600	-0.544	0.587
4	-0.031	0.027	325.200	-1.169	0.243
5	-0.019	0.029	325.500	-0.641	0.522
6	-0.020	0.031	325.700	-0.653	0.514
7	0.039	0.032	325.700	1.207	0.228
8	0.018	0.028	325.400	0.640	0.522
9	0.091	0.028	325.400	3.245	0.001**
10	-0.038	0.028	325.400	-1.366	0.173
11	0.013	0.028	325.400	0.455	0.649
12	-0.005	0.047	326.400	-0.107	0.915
13	0.000	0.029	325.400	0.007	0.994
14	0.044	0.029	325.600	1.499	0.135
15	-0.034	0.031	325.600	-1.118	0.264
16	-0.025	0.026	325.100	-0.988	0.324

Note. Deviation coding was used in this model. All β estimates relative to the grand mean. *p<0.05, two-tailed. **p<0.01, two-tailed.

Table 5. Summary of the linear mixed model examining whether channel activation was differentially predicted by RSA (standardized β) for the Emotional GNG.

Channel number	***β* estimate**	***SE***	***df***	***t***	***p***
(Intercept)	-0.089	0.042	24.858	-2.144	0.042*
1	0.007	0.037	266.689	0.198	0.843
2	0.017	0.033	266.260	0.519	0.604
3	0.035	0.034	266.479	1.030	0.304
4	-0.018	0.032	266.115	-0.551	0.582
5	-0.007	0.037	266.506	-0.196	0.845
6	-0.048	0.035	266.453	-1.361	0.175
7	-0.009	0.042	266.808	-0.205	0.838
8	-0.023	0.033	266.197	-0.675	0.500
9	0.016	0.035	266.505	0.454	0.650
10	0.020	0.035	266.455	0.568	0.571
11	0.031	0.035	266.353	0.873	0.383
12	-0.044	0.049	267.228	-0.896	0.371
13	0.026	0.037	266.499	0.702	0.483
14	-0.005	0.036	266.538	-0.145	0.885
15	0.026	0.037	266.627	0.706	0.481
16	-0.025	0.033	266.172	-0.769	0.442

Note. Deviation coding was used in this model. All β estimates relative to the grand mean. *p<0.05, two-tailed. **p<0.01, two-tailed.

Appendix A. Simple and Emotional Go/No-Go stimuli timeline

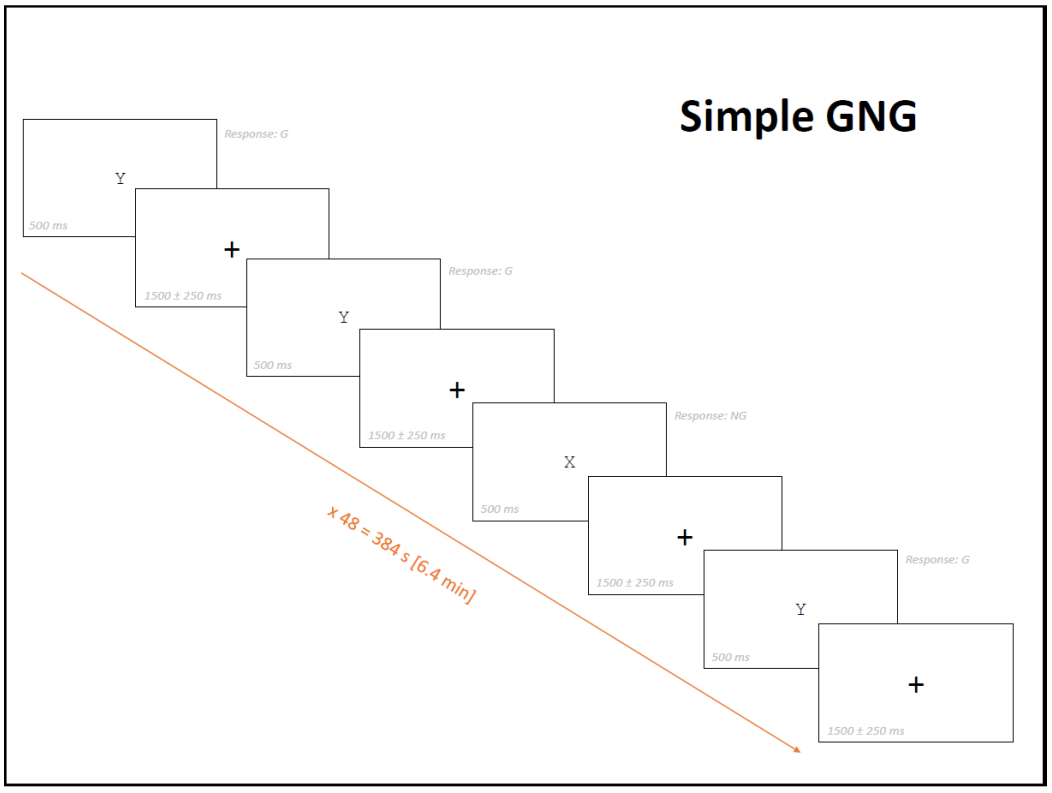

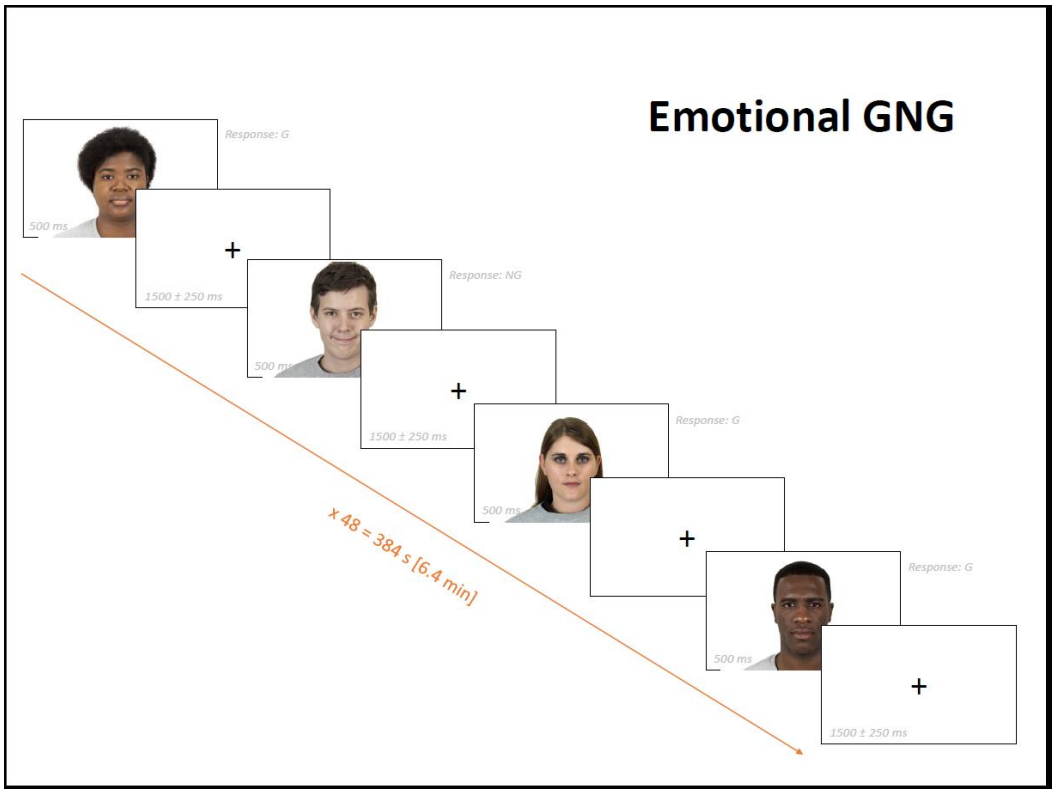

Appendix B. Supplementary Analyses

Table 6. Nonparametric paired samples t-tests comparing activation at each channel (O_2Hb) from the second half of the Simple GNG to the first half of the Simple GNG.

(Simple GNG_2 - Simple GNG_1)	***Z***	***n***	***p***
Channel 1	-2.314	24	0.021*
Channel 2	-1.493	31	0.136
Channel 3	-2.606	26	0.009*
Channel 4	-0.534	31	0.593
Channel 5	-1.731	18	0.084
Channel 6	-0.6	31	0.549
Channel 7	-1.569	29	0.117
Channel 8	-1.328	26	0.184
Channel 9	-0.725	33	0.468
Channel 10	-1.537	36	0.124
Channel 11	-0.235	31	0.814
Channel 12	-2.33	36	0.02*
Channel 13	-0.176	28	0.86
Channel 14	-1.892	24	0.058
Channel 15	-2.248	19	0.025*
Channel 16	-2.868	32	0.004*
Note. No significant differences with Bonferroni correction ($p<0.003125$); *$p<0.05$			

Table 7. Nonparametric paired samples t-tests comparing activation at each channel (O_2Hb) from the second half of the Emotional GNG to the first half of the Emotional GNG.

(Emotional GNG_2 - Emotional GNG_1)	***Z***	***n***	***p***
Channel 1	-1.672	22	0.095
Channel 2	-0.86	27	0.39
Channel 3	-1.222	24	0.222
Channel 4	-2.599	27	0.009*
Channel 5	-1.441	16	0.149
Channel 6	-2.711	27	0.007*
Channel 7	-2.485	25	0.013
Channel 8	-2.861	26	0.004*
Channel 9	-1.562	31	0.118
Channel 10	-2.743	32	0.006*
Channel 11	-2.378	29	0.017*
Channel 12	-0.776	32	0.438
Channel 13	-1.321	27	0.186
Channel 14	-1.413	22	0.158
Channel 15	-0.876	17	0.381
Channel 16	-0.47	31	0.638

Note. No significant differences with Bonferroni correction ($p<0.003125$); *$p<0.05$

Table 8. Spearman correlations (r_s) between performance metrics on the Simple GNG and β from HRV predicting activation (O_2Hb) at each channel.

		Accuracy	RT
Channel 1	r_s	0.35	0.17
	p	0.1187	0.4679
	n	21	
Channel 2	r_s	0.12	-0.07
	p	0.5658	0.7285
	n	25	
Channel 3	r_s	0.07	-0.17
	p	0.7544	0.4295
	n	25	
Channel 4	r_s	0.08	0.06
	p	0.7033	0.7894
	n	26	
Channel 5	r_s	**0.72**	**-0.7**
	p	**0.0278***	**0.0358***
	n	9	
Channel 6	r_s	0.13	-0.12
	p	0.5389	0.5765
	n	24	
Channel 7	r_s	0.21	0.23
	p	0.3331	0.2927
	n	23	
Channel 8	r_s	0.19	0.02
	p	0.4105	0.9465
	n	21	
Channel 9	r_s	**0.37**	0.15
	p	**0.0463***	0.416
	n	30	
Channel 10	r_s	0.12	-0.06
	p	0.5532	0.744
	n	28	
Channel 11	r_s	0.35	-0.05
	p	0.089	0.8056
	n	24	
Channel 12	r_s	0.08	0.04
	p	0.6776	0.84
	n	28	
Channel 13	r_s	0.19	**-0.44**
	p	0.3971	**0.034***
	n	23	
Channel 14	r_s	0.2	-0.1
	p	0.3892	0.6772
	n	20	
Channel 15	r_s	0.32	-0.02
	p	0.1767	0.9375
	n	19	
Channel 16	r_s	0.32	0.12
	p	0.1188	0.5828
	n	25	

Note. No significant correlations with Bonferroni correction. Accuracy=% correct; RT=reaction time; * p<0.05, two-tailed.

Table 9. Spearman correlations (r_s) between performance metrics on the Emotional GNG and β from HRV predicting activation (O_2Hb) at each channel.

		Accuracy	RT
Channel 1	r_s	-0.36	-0.05
	p	0.1368	0.8484
	n	18	
Channel 2	r_s	-0.38	-0.06
	p	0.0947	0.7865
	n	20	
Channel 3	r_s	-0.14	0.14
	p	0.5623	0.5565
	n	20	
Channel 4	r_s	-0.1	0.06
	p	0.686	0.7865
	n	20	
Channel 5	r_s	-0.21	0.13
	p	0.5526	0.7261
	n	10	
Channel 6	r_s	-0.17	0.15
	p	0.5011	0.559
	n	18	
Channel 7	r_s	0.01	0.03
	p	0.9744	0.8922
	n	19	
Channel 8	r_s	0.11	-0.06
	p	0.677	0.8167
	n	18	
Channel 9	r_s	0	-0.21
	p	0.9911	0.3281
	n	23	
Channel 10	r_s	-0.18	0.01
	p	0.4146	0.9702
	n	22	
Channel 11	r_s	-0.05	0.14
	p	0.8162	0.5556
	n	21	
Channel 12	r_s	-0.32	0.02
	p	0.1225	0.9293
	n	24	
Channel 13	r_s	-0.15	-0.01
	p	0.5635	0.9708
	n	18	
Channel 14	r_s	0.05	0.19
	p	0.8425	0.4237
	n	20	
Channel 15	r_s	0.07	-0.06
	p	0.8108	0.8286
	n	14	
Channel 16	r_s	-0.34	-0.14
	p	0.1172	0.5293
	n	22	

Note. Accuracy=% correct; RT=reaction time; * p<0.05, two-tailed.

References

Allen, B., Jennings, J. R., Gianaros, P. J., Thayer, J. F., & Manuck, S. B. (2015). Resting high-frequency heart rate variability is related to resting brain perfusion. *Psychophysiology, 52*(2), 277-287. doi: 10.1111/psyp.12321

Allen, J. J., Chambers, A. S., & Towers, D. N. (2007). The many metrics of cardiac chronotropy: a pragmatic primer and a brief comparison of metrics. *Biol Psychol, 74*(2), 243-262. doi: 10.1016/j.biopsycho.2006.08.005

Anderson, A. A., Smith, E., Chernomordik, V., Ardeshirpour, Y., Chowdhry, F., Thurm, A., . . . Gandjbakhche, A. H. (2014). Prefrontal cortex hemodynamics and age: a pilot study using functional near infrared spectroscopy in children. *Front Neurosci, 8*, 393. doi: 10.3389/fnins.2014.00393

Asahi, S., Okamoto, Y., Okada, G., Yamawaki, S., & Yokota, N. (2004). Negative correlation between right prefrontal activity during response inhibition and impulsiveness: a fMRI study. *Eur Arch Psychiatry Clin Neurosci, 254*(4), 245-251. doi: 10.1007/s00406-004-0488-z

Ayaz, H. (2010). *Functional Near Infrared Spectroscopy based Brain Computer Interface.* (PhD), Drexel University, Philadelphia, PA.

Ayaz, H., Shewokis, P. A., Curtin, A., Izzetoglu, M., Izzetoglu, K., & Onaral, B. (2011). Using MazeSuite and functional near infrared spectroscopy to study learning in spatial navigation. *J Vis Exp*(56). doi: 10.3791/3443

Baron-Cohen, S., Wheelwright, S., Skinner, R., Martin, J., & Clubley, E. (2001). The autism-spectrum quotient (AQ): evidence from Asperger syndrome/high-functioning autism, males and females, scientists and mathematicians. *J Autism Dev Disord, 31*(1), 5-17.

Bates, D., Maechler, M., Bolker, B., & Walker, S. (2015). Fitting Linear Mixed-Effects Models Using {lme4}. *Journal of Statistical Software, 67*(1), 1-48. doi: 10.18637/jss.v067.i01

Beissner, F., Meissner, K., Bar, K. J., & Napadow, V. (2013). The autonomic brain: an activation likelihood estimation meta-analysis for central processing of autonomic function. *J Neurosci, 33*(25), 10503-10511. doi: 10.1523/JNEUROSCI.1103-13.2013

Benarroch, E. E. (1993). The central autonomic network: functional organization, dysfunction, and perspective. *Mayo Clin Proc, 68*(10), 988-1001.

Berntson, G. G., Bigger, J. T., Jr., Eckberg, D. L., Grossman, P., Kaufmann, P. G., Malik, M., . . . van der Molen, M. W. (1997). Heart rate variability: origins, methods, and interpretive caveats. *Psychophysiology, 34*(6), 623-648.

Berntson, G. G., Cacioppo, J. T., & Quigley, K. S. (1993). Respiratory sinus arrhythmia: autonomic origins, physiological mechanisms, and psychophysiological implications. *Psychophysiology, 30*(2), 183-196.

Buckner, R. L., Andrews-Hanna, J. R., & Schacter, D. L. (2008). The brain's default network: anatomy, function, and relevance to disease. *Ann N Y Acad Sci, 1124*, 1-38. doi: 10.1196/annals.1440.011

Chang, C., Metzger, C. D., Glover, G. H., Duyn, J. H., Heinze, H. J., & Walter, M. (2013). Association between heart rate variability and fluctuations in resting-state functional connectivity. *Neuroimage, 68*, 93-104. doi: 10.1016/j.neuroimage.2012.11.038

Chen, G., Saad, Z. S., Britton, J. C., Pine, D. S., & Cox, R. W. (2013). Linear mixed-effects modeling approach to FMRI group analysis. *Neuroimage, 73*, 176-190. doi: 10.1016/j.neuroimage.2013.01.047

Criaud, M., & Boulinguez, P. (2013). Have we been asking the right questions when assessing response inhibition in go/no-go tasks with fMRI? A meta-analysis and critical review. *Neurosci Biobehav Rev, 37*(1), 11-23. doi: 10.1016/j.neubiorev.2012.11.003

Critchley, H. D., Mathias, C. J., Josephs, O., O'Doherty, J., Zanini, S., Dewar, B. K., . . . Dolan, R. J. (2003). Human cingulate cortex and autonomic control: converging neuroimaging and clinical evidence. *Brain, 126*(Pt 10), 2139-2152. doi: 10.1093/brain/awg216

Cui, X., Bray, S., Bryant, D. M., Glover, G. H., & Reiss, A. L. (2011). A quantitative comparison of NIRS and fMRI across multiple cognitive tasks. *Neuroimage, 54*(4), 2808-2821. doi: 10.1016/j.neuroimage.2010.10.069

Dajani, D. R., & Uddin, L. Q. (2015). Demystifying cognitive flexibility: Implications for clinical and developmental neuroscience. *Trends Neurosci, 38*(9), 571-578. doi: 10.1016/j.tins.2015.07.003

Dennis, J. P., & Wal, J. S. V. (2010). The Cognitive Flexibility Inventory: Instrument Development and Estimates of Reliability and Validity. *Cognitive Therapy and Research, 34*(3), 241-253. doi: 10.1007/s10608-009-9276-4

Dillo, W., Goke, A., Prox-Vagedes, V., Szycik, G. R., Roy, M., Donnerstag, F., . . . Ohlmeier, M. D. (2010). Neuronal correlates of ADHD in adults with evidence for compensation strategies--a functional MRI study with a Go/No-Go paradigm. *Ger Med Sci, 8*, Doc09. doi: 10.3205/000098

Donders, F. C. (1969). On the speed of mental processes. *Acta Psychol (Amst), 30*, 412-431.

Dowding, I., & Haufe, S. (2018). Powerful Statistical Inference for Nested Data Using Sufficient Summary Statistics. *Front Hum Neurosci, 12*, 103. doi: 10.3389/fnhum.2018.00103

Elliott, R., Rubinsztein, J. S., Sahakian, B. J., & Dolan, R. J. (2000). Selective attention to emotional stimuli in a verbal go/no-go task: an fMRI study. *Neuroreport, 11*(8), 1739-1744.

Ellis, R. J., Sollers, J. J., Edelstein, E. A., & Thayer, J. F. (2008). Data transforms for spectral analyses of heart rate variability. *Biomed Sci Instrum, 44*, 392-397.

Ferrari, M., & Quaresima, V. (2012). A brief review on the history of human functional near-infrared spectroscopy (fNIRS) development and fields of application. *Neuroimage, 63*(2), 921-935. doi: 10.1016/j.neuroimage.2012.03.049

Friedman, B. H. (2007). An autonomic flexibility-neurovisceral integration model of anxiety and cardiac vagal tone. *Biol Psychol, 74*(2), 185-199. doi: 10.1016/j.biopsycho.2005.08.009

Goldstein, M., Brendel, G., Tuescher, O., Pan, H., Epstein, J., Beutel, M., . . . Silbersweig, D. (2007). Neural substrates of the interaction of emotional stimulus processing and motor inhibitory control: an emotional linguistic go/no-go fMRI study. *Neuroimage, 36*(3), 1026-1040. doi: 10.1016/j.neuroimage.2007.01.056

Herrmann, M. J., Plichta, M. M., Ehlis, A. C., & Fallgatter, A. J. (2005). Optical topography during a Go-NoGo task assessed with multi-channel near-infrared spectroscopy. *Behav Brain Res, 160*(1), 135-140. doi: 10.1016/j.bbr.2004.11.032

Holm, S. (1979). A Simple Sequentially Rejective Multiple Test Procedure. *Scandinavian Journal of Statistics, 6*(2), 65-70.

Huppert, T. J., Diamond, S. G., Franceschini, M. A., & Boas, D. A. (2009). HomER: a review of time-series analysis methods for near-infrared spectroscopy of the brain. *Appl Opt, 48*(10), D280-298.

Irani, F., Platek, S. M., Bunce, S., Ruocco, A. C., & Chute, D. (2007). Functional near infrared spectroscopy (fNIRS): an emerging neuroimaging technology with important applications

for the study of brain disorders. *Clin Neuropsychol, 21*(1), 9-37. doi: 10.1080/13854040600910018

Janig, W., & Habler, H. J. (2000). Specificity in the organization of the autonomic nervous system: a basis for precise neural regulation of homeostatic and protective body functions. *Prog Brain Res, 122*, 351-367.

Jennings, J. R., Allen, B., Gianaros, P. J., Thayer, J. F., & Manuck, S. B. (2015). Focusing neurovisceral integration: cognition, heart rate variability, and cerebral blood flow. *Psychophysiology, 52*(2), 214-224. doi: 10.1111/psyp.12319

Jennings, J. R., Kamarck, T., Stewart, C., Eddy, M., & Johnson, P. (1992). Alternate cardiovascular baseline assessment techniques: vanilla or resting baseline. *Psychophysiology, 29*(6), 742-750.

Kuznetsova, A., Brockhoff, P. B., & Christensen, R. H. B. (2017). lmerTest Package: Tests in Linear Mixed Effects Models. *Journal of Statistical Software, 82*(13), 1-26. doi: 10.18637/jss.v082.i13

Lee, H. J., Yost, B. P., & Telch, M. J. (2009). Differential performance on the go/no-go task as a function of the autogenous-reactive taxonomy of obsessions: findings from a non-treatment seeking sample. *Behav Res Ther, 47*(4), 294-300. doi: 10.1016/j.brat.2009.01.002

Lloyd-Fox, S., Blasi, A., & Elwell, C. E. (2010). Illuminating the developing brain: the past, present and future of functional near infrared spectroscopy. *Neurosci Biobehav Rev, 34*(3), 269-284. doi: 10.1016/j.neubiorev.2009.07.008

Ma, D. S., Correll, J., & Wittenbrink, B. (2015). The Chicago face database: A free stimulus set of faces and norming data. *Behav Res Methods, 47*(4), 1122-1135. doi: 10.3758/s13428-014-0532-5

Monti, M. M. (2011). Statistical Analysis of fMRI Time-Series: A Critical Review of the GLM Approach. *Front Hum Neurosci, 5*, 28. doi: 10.3389/fnhum.2011.00028

Mostofsky, S. H., Schafer, J. G., Abrams, M. T., Goldberg, M. C., Flower, A. A., Boyce, A., . . . Pekar, J. J. (2003). fMRI evidence that the neural basis of response inhibition is task-dependent. *Brain Res Cogn Brain Res, 17*(2), 419-430.

Napadow, V., Dhond, R., Conti, G., Makris, N., Brown, E. N., & Barbieri, R. (2008). Brain correlates of autonomic modulation: combining heart rate variability with fMRI. *Neuroimage, 42*(1), 169-177. doi: 10.1016/j.neuroimage.2008.04.238

R Core Team. (2017). R: A language and environment for statistical computing. Vienna, Austria.

Rodrigo, A. H., Domenico, S. I., Ayaz, H., Gulrajani, S., Lam, J., & Ruocco, A. C. (2014). Differentiating functions of the lateral and medial prefrontal cortex in motor response inhibition. *Neuroimage, 85 Pt 1*, 423-431. doi: 10.1016/j.neuroimage.2013.01.059

Ruzich, E., Allison, C., Smith, P., Watson, P., Auyeung, B., Ring, H., & Baron-Cohen, S. (2015). Measuring autistic traits in the general population: a systematic review of the Autism-Spectrum Quotient (AQ) in a nonclinical population sample of 6,900 typical adult males and females. *Mol Autism, 6*, 2. doi: 10.1186/2040-2392-6-2

Saul, J. P. (1990). Beat-to-Beat Variations of Heart-Rate Reflect Modulation of Cardiac Autonomic Outflow. *News in Physiological Sciences, 5*, 32-37.

Scarpina, F., & Tagini, S. (2017). The Stroop Color and Word Test. *Front Psychol, 8*, 557. doi: 10.3389/fpsyg.2017.00557

Schneider, W., Eschman, A., & Zuccolotto, A. (2002). *E-Prime User's Guide.* Pittsburgh: Psychology Software Tools Inc. .

Schulz, K. P., Fan, J., Magidina, O., Marks, D. J., Hahn, B., & Halperin, J. M. (2007). Does the emotional go/no-go task really measure behavioral inhibition? Convergence with measures on a non-emotional analog. *Arch Clin Neuropsychol, 22*(2), 151-160. doi: 10.1016/j.acn.2006.12.001

Simmonds, D. J., Pekar, J. J., & Mostofsky, S. H. (2008). Meta-analysis of Go/No-go tasks demonstrating that fMRI activation associated with response inhibition is task-dependent. *Neuropsychologia, 46*(1), 224-232. doi: 10.1016/j.neuropsychologia.2007.07.015

Swick, D., Ashley, V., & Turken, U. (2011). Are the neural correlates of stopping and not going identical? Quantitative meta-analysis of two response inhibition tasks. *Neuroimage, 56*(3), 1655-1665. doi: 10.1016/j.neuroimage.2011.02.070

Takahashi, N., Kuriyama, A., Kanazawa, H., Takahashi, Y., & Nakayama, T. (2017). Validity of spectral analysis based on heart rate variability from 1-minute or less ECG recordings. *Pacing Clin Electrophysiol, 40*(9), 1004-1009. doi: 10.1111/pace.13138

Task Force. (1996). Heart rate variability. Standards of measurement, physiological interpretation, and clinical use. Task Force of the European Society of Cardiology and the North American Society of Pacing and Electrophysiology. *Eur Heart J, 17*(3), 354-381.

Thayer, J. F., Ahs, F., Fredrikson, M., Sollers, J. J., 3rd, & Wager, T. D. (2012). A meta-analysis of heart rate variability and neuroimaging studies: implications for heart rate variability as a marker of stress and health. *Neurosci Biobehav Rev, 36*(2), 747-756. doi: 10.1016/j.neubiorev.2011.11.009

Thayer, J. F., Hansen, A. L., Saus-Rose, E., & Johnsen, B. H. (2009). Heart rate variability, prefrontal neural function, and cognitive performance: the neurovisceral integration perspective on self-regulation, adaptation, and health. *Ann Behav Med, 37*(2), 141-153. doi: 10.1007/s12160-009-9101-z

Thayer, J. F., & Lane, R. D. (2000). A model of neurovisceral integration in emotion regulation and dysregulation. *J Affect Disord, 61*(3), 201-216.

Uzefovsky, F., Allison, C., Smith, P., & Baron-Cohen, S. (2016). Brief Report: The Go/No-Go Task Online: Inhibitory Control Deficits in Autism in a Large Sample. *J Autism Dev Disord, 46*(8), 2774-2779. doi: 10.1007/s10803-016-2788-3

Warnes, G. R., Bolker, B., Bonebakker, L., Gentleman, R., Liaw, W. H. A., Lumley, T., . . . Venables, B. (2016). gplots: Various R Programming Tools for Plotting Data. Retrieved from https://CRAN.R-project.org/package=gplots

Watanabe, J., Sugiura, M., Sato, K., Sato, Y., Maeda, Y., Matsue, Y., . . . Kawashima, R. (2002). The human prefrontal and parietal association cortices are involved in NO-GO performances: an event-related fMRI study. *Neuroimage, 17*(3), 1207-1216.